



# Removal of Ciprofloxacin from Water using Adsorption, UV Photolysis and UV/H<sub>2</sub>O<sub>2</sub> Degradation

Major Qualifying Project completed in partial fulfillment  
Of the Bachelor of Science Degree at  
Worcester Polytechnic Institute, Worcester, MA

Submitted by:

Melissa Roma  
Marc Weller  
Samantha Wentzell

Professors John Bergendahl and Robert Thompson, faculty advisors

April 28, 2011

This report represents the work of three WPI undergraduate students submitted to the faculty as evidence of a degree requirement. WPI routinely publishes these reports on its web site without editorial or peer review

## **Abstract**

The objective of this project was to study removal and degradation of ciprofloxacin (CIP) from water utilizing three treatment methods at pH 3, 7, and 10. Treatments included ultraviolet light (UV) photolysis, UV with hydrogen peroxide (H<sub>2</sub>O<sub>2</sub>) degradation, and adsorption to two types of granular activated carbons (GAC). The concentration of CIP remaining after treatment was quantified using a UV spectrophotometer. Results showed that all treatment methods evaluated were capable of removing high concentrations of CIP from water. The addition of H<sub>2</sub>O<sub>2</sub> to UV treatment doubled the rate of CIP degradation that occurred using UV photolysis by itself. Both UV treatments were found to be most successful at pH 3. Experiments also showed that CIP had a higher affinity for adsorption to F200 GAC than F600 GAC. All adsorption treatments were most successful at pH 7.

## **Acknowledgements**

We would like to thank our advisors, Professors John A. Bergendahl and Robert W. Thompson for their ongoing support and feedback throughout the year. Also, special thanks to Justyna Krupa of Calgon Carbon Corporation for her activated carbon recommendations and to Don Pellegrino and Huong Nguyen for their help in the laboratory.

## Table of Contents

|   |    |
|---|----|
| Abstract .....  | i  |
| Acknowledgements .....  | ii |
| Table of Tables .....   | v  |
| Table of Figures .....  | v  |
| Chapter 1: Introduction .....   | 1  |
| Chapter 2: Background .....   | 4  |
| 2.1 Compounds of Emerging Concern.....                                    | 4  |
| 2.1.1 Ciprofloxacin .....   | 6  |
| 2.2 CIP in the Environment .....  | 8  |
| 2.2.1 Occurrence .....  | 8  |
| 2.2.2 Bacterial Resistance .....  | 10 |
| 2.2.3 Environmental Risks of CIP .....                                    | 12 |
| 2.3 Potential Treatment Methods.....                                      | 13 |
| 2.3.1 Adsorption.....   | 13 |
| 2.3.2 Advanced Oxidation Treatments (AOPs) .....                          | 17 |
| 2.3.3 Additional AOPs .....   | 21 |
| 2.4 Summary .....   | 24 |
| Chapter 3: Methodology .....  | 25 |
| 3.1 Sample Preparation .....  | 25 |
| 3.2 Measuring Sample Absorbance .....                                     | 25 |
| 3.3 Ciprofloxacin Concentration Standard Curves with Detection Limit..... | 25 |
| 3.4 Ultraviolet Treatment.....  | 26 |
| 3.4.1 UV Photolysis: 75 minute exposure time .....                        | 26 |
| 3.4.2 UV Time Trials .....  | 27 |
| 3.4.3 Ultraviolet Treatment with Addition of Hydrogen Peroxide .....      | 27 |
| 3.5 Adsorption Treatment .....  | 27 |
| 3.5.1 Adsorption Equilibrium Trials .....                                 | 28 |
| 3.5.2 Adsorption Time Trials – Kinetics.....                              | 28 |
| Chapter 4: Results and Discussion.....                                    | 29 |
| 4.1 Calibration Curves .....  | 29 |
| 4.2 UV Degradation.....   | 30 |

|   |    |
|---|----|
| 4.2.1 Determination of Effective UV Wavelength.....                       | 30 |
| 4.2.2 UV Photolysis .....   | 30 |
| 4.2.3 UV/H <sub>2</sub> O <sub>2</sub> Degradation.....                   | 32 |
| 4.2.4 UV and UV/H <sub>2</sub> O <sub>2</sub> Degradation Comparison..... | 35 |
| 4.3 Adsorption.....   | 36 |
| 4.3.1 Adsorption Isotherms .....  | 36 |
| 4.3.2 Adsorption Kinetics .....   | 39 |
| Chapter 5: Conclusions and Recommendations.....                           | 42 |
| Bibliography .....  | 43 |
| Appendix A –Glossary of Terms .....                                       | 49 |
| Appendix B - Raw Data.....  | 50 |
| Calibration Curves .....  | 50 |
| UV Photolysis at 365nm .....  | 50 |
| UV Photolysis Kinetics at 254 nm.....                                     | 50 |
| UV/H <sub>2</sub> O <sub>2</sub> Degradation.....                         | 51 |
| UV/H <sub>2</sub> O <sub>2</sub> Degradation – Kinetics .....             | 52 |
| Adsorption - F600 Isotherm.....   | 53 |
| Adsorption – F200 Isotherm .....  | 54 |
| Adsorption - F600 Kinetics.....   | 55 |
| Adsorption - F200 Kinetics.....   | 56 |
| Appendix C: Sample Calculations .....                                     | 58 |
| Detection Limit .....   | 58 |
| Adsorption Isotherms.....   | 59 |
| F600 .....  | 59 |
| F200 .....  | 60 |
| Adsorption Kinetics .....   | 61 |
| F600 .....  | 61 |
| F200 .....  | 62 |

## Table of Tables

|  |    |
|--|----|
| Table 1: UV wavelength comparison.....   | 30 |
| Table 2: UV degradation with varying ratios of H <sub>2</sub> O <sub>2</sub> /CIP..... | 33 |
| Table 3: Calibration Curves.....   | 50 |
| Table 4: UV Photolysis at 365 nm.....  | 50 |
| Table 5: UV Photolysis Kinetics at pH 3.....   | 50 |
| Table 6: UV Photolysis Kinetics at pH 7.....   | 51 |
| Table 7: UV Photolysis Kinetics at pH 10.....  | 51 |
| Table 8: UV /H <sub>2</sub> O <sub>2</sub> Degradation at pH 3.....                    | 51 |
| Table 9: UV /H <sub>2</sub> O <sub>2</sub> Degradation at pH 7.....                    | 52 |
| Table 10: UV /H <sub>2</sub> O <sub>2</sub> Degradation at pH 10.....                  | 52 |
| Table 11: UV /H <sub>2</sub> O <sub>2</sub> Degradation Kinetics at pH 3.....          | 52 |
| Table 12: UV /H <sub>2</sub> O <sub>2</sub> Degradation Kinetics at pH 7.....          | 53 |
| Table 13: UV /H <sub>2</sub> O <sub>2</sub> Degradation Kinetics at pH 10.....         | 53 |
| Table 14: F600 Isotherm at pH 3.....   | 53 |
| Table 15: F600 Isotherm at pH 7.....   | 54 |
| Table 16: F600 Isotherm at pH 10.....  | 54 |
| Table 17: F200 Isotherm at pH 3.....   | 54 |
| Table 18: F200 Isotherm at pH 7.....   | 55 |
| Table 19: F200 Isotherm at pH 10.....  | 55 |
| Table 20: F600 Adsorption Kinetics at pH 3.....  | 55 |
| Table 21: F600 Adsorption Kinetics at pH 7.....  | 56 |
| Table 22: F600 Adsorption Kinetics at pH 10.....                                       | 56 |
| Table 23: F200 Adsorption Kinetics at pH 3.....  | 56 |
| Table 24: F200 Adsorption Kinetics at pH 7.....  | 57 |
| Table 25: F200 Adsorption Kinetics at pH 10.....                                       | 57 |
| Table 26: Detection Limit Data.....  | 58 |
| Table 27: t-Test: Paired Two Sample for Means.....                                     | 58 |

## Table of Figures

|  |    |
|--|----|
| Figure 1: Molecular Structure of CIP.....  | 2  |
| Figure 2: Main Pathways for PPCPs Entering the Environment.....                            | 5  |
| Figure 3: Molecular Structure of CIP.....  | 7  |
| Figure 4: Acid-Base Speciation of CIP.....   | 7  |
| Figure 5: Hypothetical Antibiotic Dose Relationship for Normal and Resistant Bacteria..... | 10 |
| Figure 6: FQ Mechanism of UV Degradation During Photolysis.....                            | 19 |
| Figure 7: UV Treatment Glass Tube and Light Apparatus.....                                 | 26 |
| Figure 8: Calibration curves for UV spectrometer at 280 nm.....                            | 29 |

|  |    |
|--|----|
| Figure 9: UV photolysis degradation at 254 nm .....                                    | 31 |
| Figure 10: 1st order UV Photolysis Kinetics .....                                      | 32 |
| Figure 11: UV/H <sub>2</sub> O <sub>2</sub> degradation at 254 nm.....                 | 34 |
| Figure 12: UV/H <sub>2</sub> O <sub>2</sub> degradation at 254 nm.....                 | 35 |
| Figure 13: UV and UV/H <sub>2</sub> O <sub>2</sub> Degradation at 254 nm and pH 3..... | 36 |
| Figure 14: F600 Adsorption Isotherm.....   | 37 |
| Figure 15: F200 Adsorption Isotherm.....   | 38 |
| Figure 16: F600 Adsorption Kinetics.....   | 39 |
| Figure 17: F200 Adsorption Kinetics.....   | 40 |
| Figure 18: Comparison of Adsorption Kinetics at pH 7 for F600 and F200 .....           | 41 |
| Figure 19: F600 Freundlich Isotherm .....  | 59 |
| Figure 20: F600 Langmuir Isotherm.....   | 59 |
| Figure 21: F200 Freundlich Isotherm .....  | 60 |
| Figure 22: F200 Langmuir Isotherm.....   | 60 |
| Figure 23: F600 1st Order Kinetics.....  | 61 |
| Figure 24: F600 2nd Order Kinetics .....   | 61 |
| Figure 25: F200 1st Order Kinetics.....  | 62 |
| Figure 26: F200 2nd Order Kinetics .....   | 62 |
| Figure 27: F200 Data Sheet .....   | 63 |
| Figure 28: F600 Data Sheet .....   | 64 |

## Chapter 1: Introduction

The rapid growth of the world's population has created a corresponding increase in the demand for the Earth's limited supply of freshwater. Thus, protecting the supply of our water and addressing concerns such as toxicity and the presence of chemicals that may have potential long term adverse human and ecological effects has become an important issue. Research in the past 30 years has shown pharmaceuticals and personal care products (PPCPs) as emerging organic micro-contaminants due to their extensive use in human and veterinary medicine and their increasing occurrence in the aquatic environment (Avisar et al., 2009). The global market for pharmaceuticals has been estimated between 100,000-200,000 tons/year (Zucatto et al., 2010). PPCPs enter the environment at low concentrations primarily as metabolites excreted by humans and animals or in effluents that are disposed into wastewater from hospitals, pharmacies, and chemical manufacturing facilities (Nikolaou et al., 2007). Once these compounds reach wastewater treatment plants (WWTPs), they are not completely removed and residual concentrations of these chemicals are frequently discharged in the treated effluent. Current WWTPs have technologies that discharge water that meets regulatory standards, but the list of the important classes of contaminants that are not regulated in drinking and other waters remains extensive. Until recently, this has been due primarily to the non-availability of analytical instruments that can identify low concentrations (ng/L - µg/L) of those contaminants. Therefore, while scientists catch up with the research, low concentrations of pollutants continue to be released into the environment that can contaminate surface water, seawater, and groundwater (Avisar et al., 2009) and have a negative environmental impacts.

Fluoroquinolones (FQs) are a class of broad spectrum antibiotics that are commonly used in both human and veterinary medicine. They inhibit key bacterial enzymes, such as DNA gyrase and topoisomerase IV, that are involved with unwinding the DNA helix for replication and transcription. FQs are of concern because they are widely used in Europe and the USA and are not readily biodegradable by microorganisms (Robinson et al., 2004). They are not completely metabolized in the human body and approximately 20-90% of FQs ingested are excreted in their pharmacologically active forms, which leads to significant loads being discharged into domestic sewage (Paul et al., 2010). Furthermore, conventional wastewater treatment in WWTPs generally



result in prolonged exposure of wastewater-borne bacteria to higher concentrations of FQs that are not present in treated effluents because of extended biomass solid retention times at which secondary clarifiers usually operate. This is important because different FQs have been found in secondary wastewater effluents at concentrations close to minimal inhibitory concentrations (MICs) for various bacterial strains. Extended exposure of bacterial communities to MIC levels of FQs (and other antibacterial compounds) can result in an environment where the evolution of low-level antibacterial resistance is favored in the affected bacterial communities (Paul et al., 2010).

Ciprofloxacin (CIP), a second generation FQ and one of the most prescribed drugs in the world, has been widely researched because it has been regularly found in wastewater at MIC levels that could induce bacterial resistance. CIP is a broad spectrum antibiotic that is effective against gram-positive and gram-negative bacteria. It was recommended during the anthrax outbreak in 2001 and has also been used to target biological agents of Legionnaire's disease and typhoid. It also belongs to a class of powerful FQs that have been linked to serious side effects which include ruptured tendons and neurological damage resulting from seizures (CBWInfo.com, 2005). Figure 1 shows the basic structure of CIP.

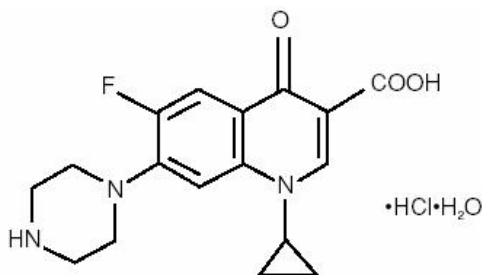


Figure 1: Molecular Structure of CIP (DailyMed, 2008)

Taking completed research into consideration, it can be concluded that there is an incentive for removing CIP, as well as other FQs and pharmaceuticals, from wastewater. One means of achieving this objective is implementing treatment technologies capable of selectively and efficiently eliminating the biological activities of antibacterial compounds. Many studies have shown that advanced oxidation processes (AOPs) and adsorption applications are viable treatment methods for degrading or completely removing CIP from water and wastewater. The most researched AOPs are ozonation, sonification, photolysis, and heterogeneous photocatalysis.

Various studies have shown that CIP is susceptible to direct photochemical transformations by exposure to direct ultraviolet (UV) light and by adding photocatalytic reagents such as hydrogen peroxide( $H_2O_2$ ), and titanium dioxide( $TiO_2$ ), to aqueous solutions (Avisar et al, 2010; Paul et al., 2010). Research has also been conducted for CIP adsorption onto water sediment, soil and sludge (Carmosini et al., 2009).

Despite all of the research that has been conducted, there have been few studies of treatment methods that have analyzed pH modification of water followed by photolytic treatment or adsorption onto activated carbon. Adjusting the pH of water leads to structural modifications of CIP and these changes could enhance degradation by direct photolysis via UV light and photocatalysis. There were also few studies regarding adsorption of CIP onto activated carbons. CIP is a large molecule, so adsorption onto activated carbons appears to be a promising treatment method. Overall, few researchers have analyzed degradation of CIP by AOPs; therefore additional research must be completed, addressing a wide range of parameters for AOPs.

The purpose of this project was to investigate treatment methods for removing CIP from E-pure water, which is reagent-grade bacteria free water. The group accomplished this goal by ascertaining US and international treatment methods for removing CIP and other pharmaceuticals from water and wastewater, researching potential pathways for pharmaceuticals to enter the water supply, the environmental risk and the long term effects they pose to organisms (including humans), and the current technologies that are being utilized. The team then evaluated the current treatment methods performed by experts in the field in order to identify the gaps in their experimental results and then help to fill those gaps through a series of UV photolysis, UV/ $H_2O_2$ , and adsorption experiments.

## Chapter 2: Background

This chapter will provide an overview of the research that has been completed pertaining to the occurrence, environmental concerns, and treatment technologies for CIP. First, the concern for emerging compounds is introduced in order to establish the concern for the potential risks that CIP and other pharmaceutically active compounds (PhACs) pose to the environment. Next, the structure and acid-base speciation chemistry of CIP will be discussed. Occurrence, bacterial resistance, and the environmental risks of CIP will then be highlighted. Finally, adsorption, UV photolysis, and UV/H<sub>2</sub>O<sub>2</sub> will be described because they are the treatment methods that were analyzed in this project. Other AOPs are mentioned as potentially successful methods of treatment; although they were not tested in this study.

### 2.1 Compounds of Emerging Concern

For more than 70 years, researchers have reported that various synthetic and natural compounds can affect the balance of normal hormonal functions in animals (U.S. Department of the Interior Bureau of Reclamation, 2009). These compounds are called endocrine disrupting chemicals (EDCs) and have been linked to many adverse effects in humans and wildlife. The United States Environmental Protection Agency (USEPA) defines EDCs as agents which interfere with the synthesis, secretion, transport, binding, action or elimination of natural hormones in the body that are responsible for the maintenance of homeostasis, reproduction, development, and behavior. The majority of EDCs are synthetically produced like surfactants, pesticides, pharmaceuticals, and phthalates, but others occur naturally such as estrone and 17 $\beta$ -estradiol (Nikolaou et al., 2007). Although they do not have direct effects on humans or other living organisms, EDCs indirectly disrupt the endocrine system which controls the body's function and results in either the suppression or production of excessive amounts of hormones. Opinions vary between scientists on whether or not there is disputable evidence on the effects of EDCs, but there is an agreement on their properties. Stronger endocrine disruption occurs when more than one compound simultaneously exists even though they may have insignificant individual effects and EDCs are soluble in adipose tissues and collect over time in the body (Caliman et al., 2009).

Recently, PhACs and personal care products (PCPs) have been discovered in ground and surface waters. These compounds have been detected at trace concentrations that can induce

various ecological impacts on aquatic organisms as well as induce endocrine disrupting effects (Caliman et al., 2009). These compounds, combined with EDCs, have been grouped with other emerging contaminants (such as metals and nitrosamines) and are referred to as compounds of emerging concern (CECs). In particular, pharmaceuticals and personal care products (PPCPs) have become an emerging environmental problem because they are being used more extensively in human and veterinary medicines, soaps, detergents, and hair sprays, which are released into the water and environment daily. A problem exists with ecotoxicological effects of PPCPs because to date many of these compounds have not been classified as having human health effects at low dose concentrations (U.S. Department of the Interior Bureau of Reclamation, 2009). Until recently, this lack of information has resulted from inefficient analytical standards and technology for identifying compounds at low concentration levels. According to USEPA, there are approximately 38,000 chemicals and heavy metals that have been catalogued for having adverse human health effects and approximately 87,000 more chemicals still need to be tested. PPCPs enter the environment from various sources which include WWTP effluents, leakage from septic tanks or landfill sites, surface water run-off, and direct discharge in waters. Figure 2 shows the primary pathways for PPCPs entering the environment. Veterinary drugs are transported to groundwater from livestock run-off and leaching and human pharmaceuticals enter the water system from ingestion followed by excretion in the forms of non-metabolized parent compounds or metabolites (Nikolaou et al., 2007).

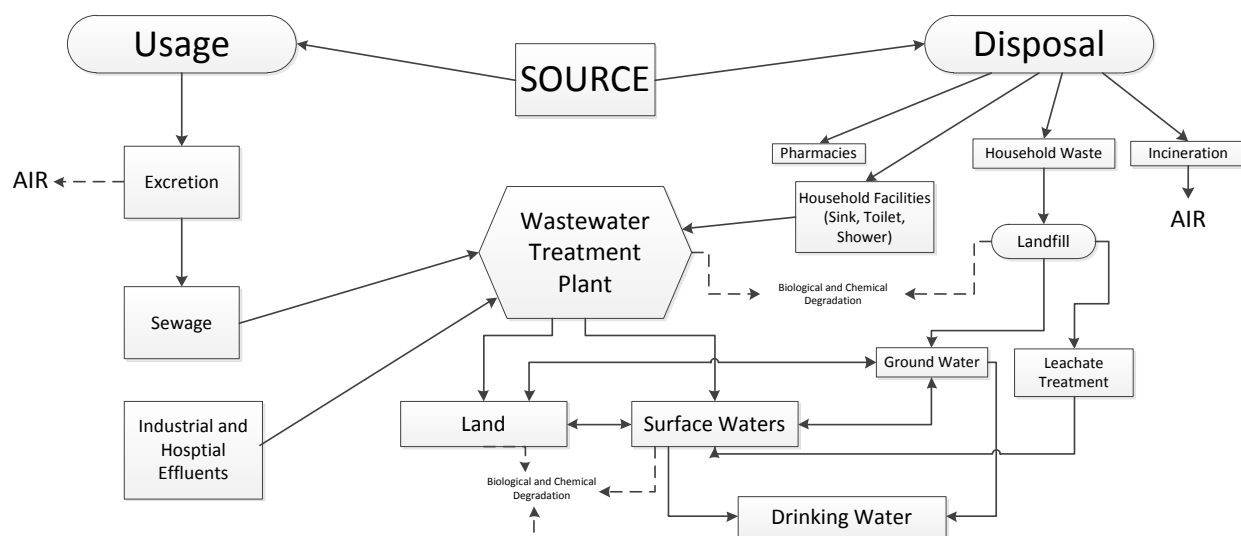


**Figure 2: Main Pathways for PPCPs Entering the Environment (Adapted from Nikolaou et al., 2007)**

Different types of environments where EDCs are found such as groundwater and surface water as well as the type of treatment plant (WWTP, drinking water) can influence various transformations and the products formed.

The rapid development of analytical technologies in the recent years has allowed scientists to investigate pharmaceuticals at trace concentrations. Yet, information on the fate, transformation pathways, toxic effects, and degradation byproducts is still limited due to the lack of inventory on the pharmaceuticals. The more recent primary methods for detecting and identifying chemicals are GC-MS, LC-MS-(MS), and HPLC, but these still present a series of disadvantages. The drawbacks include difficulty in mastering the technique, expensive cost of equipment, time consuming analysis, necessity of large sample sizes, and the requirement of specific procedures for measurement of EDCs in complex samples.

Continuous population growth and urbanization has led to more wastewater discharged into the environment. Thus, increasing amounts and diversity of PPCPs are entering the ecosystem causing environmental risks such as bacterial resistance to organisms. The widely researched antibiotic CIP has been investigated for occurrence, bacterial resistance, and experimented for degradation in water and wastewater using AOPs.

### **2.1.1 Ciprofloxacin**

CIP is a second generation synthetic chemotherapeutic antibiotic of the fluoroquinolone drug class. The drug kills bacteria by interfering with enzymes that stop DNA and protein synthesis. It is a proven treatment for many bacterial infections such as bone and joint infections, acute uncomplicated cystitis in females, lower respiratory tract infections, and in some cases urinary tract infections. CIP was once considered an antibiotic of last resort for particular infections, but now it is one of the most widely distributed antibiotics in the United States and Europe (Bhandari et al., 2008).

CIP's complete chemical name is 1-cyclopropyl-6-fluoro-1, 4-dihydro-4-oxo-7-(1-piperazinyl)-3-quinolinecarboxylic acid. As shown in Figure 3, a cyclopropyl group is attached the nitrogen atom at position 1. At position 7, the piperazine moiety is attached to the second nitrogen atom. The moiety is directly responsible for the antimicrobial activity of the fluoroquinolone molecule. The two fused six-member benzene rings is the quinolone molecule

and, along with the piperazine substituent, is an essential attack site for oxidation (Melo et al., n.d.).

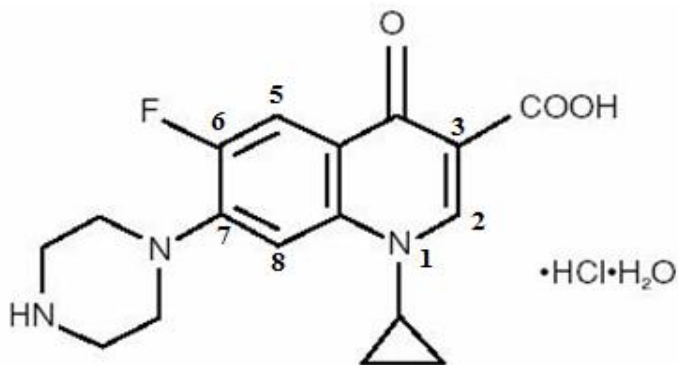


Figure 3: Molecular Structure of CIP (DailyMed, 2008)

CIP has a molecular weight of 173.168 g/mol. At standard temperature and pressure CIP exists in the solid phase with a melting point of 278.5°C, and has an approximate solubility of 350 mg/L in water. The reported values of pKa for CIP are 5.5 and 7.7. Figure 4 shows the acid-base speciation of CIP.

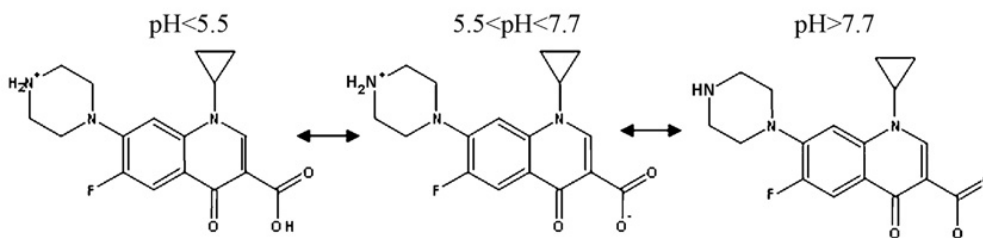


Figure 4: Acid-Base Speciation of CIP (Avisar et al., 2010)

In an acidic solution ( $\text{pH} < 5.5$ ) CIP is protonated and thus the cationic form is dominant. In a relatively neutral solution, ( $5.5 < \text{pH} < 7.7$ ) the hydrogen is removed from the carboxyl group, making the zwitterionic form of CIP dominant. In a basic solution with a  $\text{pH} > 7.7$ , the hydrogen attached to the nitrogen in the piperazine moiety is deprotonated and the anionic form of CIP becomes most prevalent. These different forms have created a cause for concern since CIP is found in wastewaters in mixtures of different antibiotics and at varying pH's. Therefore, it is

essential to analyze treatment methods in all three pH ranges to ensure that the degree of protonation does not adversely affect the treatment being implemented (Wu et al., 2010).

## **2.2 CIP in the Environment**

It is estimated that 100,000-200,000 tons of antibiotics are consumed in the global market each year. These pharmaceuticals enter the world's water systems through various sources such as hospital effluents, human sewage, and discharge from industrial pharmaceutical plants (Zuccato et al., 2010). CIP is commonly found in many of these sources and its widespread occurrence has led to bacterial resistant organisms in WWTP sewage sludge (Carmosini et al., 2009). CIP resistant organisms and low concentrations of residual CIP in WWTP sludge released into the environment without regulation are risks that are being addressed because of their potential environmental hazards.

### **2.2.1 Occurrence**

The majority of the occurrence studies have been conducted in Italy, Spain, Switzerland, China, USA, and Germany. The studies identified pharmaceuticals that could cause an environmental risk and are not readily degraded in WWTPs (Caliman et al., 2009). CIP has been identified in almost all of these studies ranging in concentrations as low as 0.02µg/L (Plosz et al., 2010) to mg/L ranges from a variety of sources that include WWTPs, surface waters, ground waters, and seawaters. In general, trace levels of CIP were found in the majority of water bodies, including lakes and rivers, but was more prevalent in areas with a high volume of pharmaceutical production and major WWTPs. Countries with less sophisticated treatment methods were also found to have higher levels of CIP and other pharmaceuticals in their water supplies. The primary concerns with the occurrence of CIP and other pharmaceuticals at trace levels are the risks they pose for aquatic ecosystems and whether their presence in natural waters contributes to the spread of antibiotic resistance in microorganisms.

Kolpin et al. (2002) used five newly developed analytical methods to measure concentrations of 95 organic contaminants in wastewater from 139 streams across 30 states during 1999 and 2000. The samples were selected where contaminants have the highest probability of being identified – downstream of urbanization and livestock production. Contaminants were found in approximately 80% of the streams. CIP was analyzed by tandem

and single quadrupole, LC/MS-ESI (+) and identified in 115 stream samples with a frequency of 2.4% ranging in concentrations of 0.02-0.03 $\mu\text{g/L}$ . The low frequency of detection was justified by the apparent affinity of CIP to adsorb to sediment in the individual sample sites.

Giger et al. (2003) showed that trace concentrations of CIP and other antibiotics occur in hospital and municipal wastewaters and in the aquatic environment. CIP was substantially eliminated in the WWTP with approximately 80-90% removed by sorption transfer to sewage sludge (digested sludge contains FQs at mg/kg levels) and the sediments in the Glatt River removes an additional 66% of CIP. The results suggest sewage sludge as the main reservoir for CIP and other FQs which indicate the importance of sludge management in determining whether or not most of the human-excreted FQs enter the environment.

Bhandari et al. (2008) evaluated the occurrence of CIP, sulfamethoxazole, and azithromycin in various aqueous streams for four municipal WWTPs at four different times of the year in the Midwestern, United States. Solid Phase Extraction (SPE) followed by HPLC/UV-FL was used to extract, separate, and quantify CIP. Compared to literature values researched by the author, the concentration of CIP remained similar. The concentration of CIP in raw wastewater was 1.44 $\mu\text{g/L}$  and 0.59 $\mu\text{g/L}$  in the WWTP effluent. CIP concentrations were significantly higher in the summer than in the winter.

Fick et al. (2009) performed an investigation on an area in India with major pharmaceutical production. The WWTP treated 1,500  $\text{m}^3/\text{day}$  of wastewater from 90 bulk drug manufacturers. The plant used several methods of treatment, including biological treatment and adsorption. The rivers upstream of the plant contained approximately 12,000 ng/L CIP. After treatment, CIP was measured at several distances downstream. Approximately 2,500  $\mu\text{g/L}$  of CIP was measured 150 m downstream, 1,100  $\mu\text{g/L}$  of CIP was measured at a distance of 4 km downstream, and 10,000 ng/L of CIP was measured 30 km downstream from the treatment facility. The studies confirm that WWTPs do not consistently or efficiently remove CIP from the influents, and thus CIP is released into water bodies across the world.

Plosz et al. (2010) conducted a study to compare the occurrence of CIP in Brazilian hospital effluents and WWTP effluents to already known occurrences of CIP in Europe and the United States. In the United States, the average CIP in WWTP influents is 0.15  $\mu\text{g/L}$ , the average in effluent is 0.06  $\mu\text{g/L}$ , and the average amount in surface water is 0.02  $\mu\text{g/L}$ . The study found



that in Brazil, there was a high amount of CIP in surface water, because the hospitals and WWTPs often lacked proper removal techniques, or by-passed treatment altogether.

### 2.2.2 Bacterial Resistance

Antibiotics and pharmaceuticals have improved public health and quality of life worldwide, but infections caused by antibiotic resistant bacteria have emerged as a major public health issue. Infections caused by multiple antibiotic resistant organisms in hospitals have continued to increase. Resistant bacteria have also been found throughout the world in various surface and groundwaters (Nagulapally et al., 2008). The widespread occurrence of contaminants in the environment poses a significant public concern because long term, low level (ng/L - µg/L) exposures to antimicrobials has a potential to cause broad antibacterial resistance in bacteria.

Antibiotics exhibit a dose-response relationship in normal bacteria cultures. Figure 5 shows the hypothetical antibiotic dose-response relationship by a solid line for normal bacteria and a dashed line for resistant bacteria.

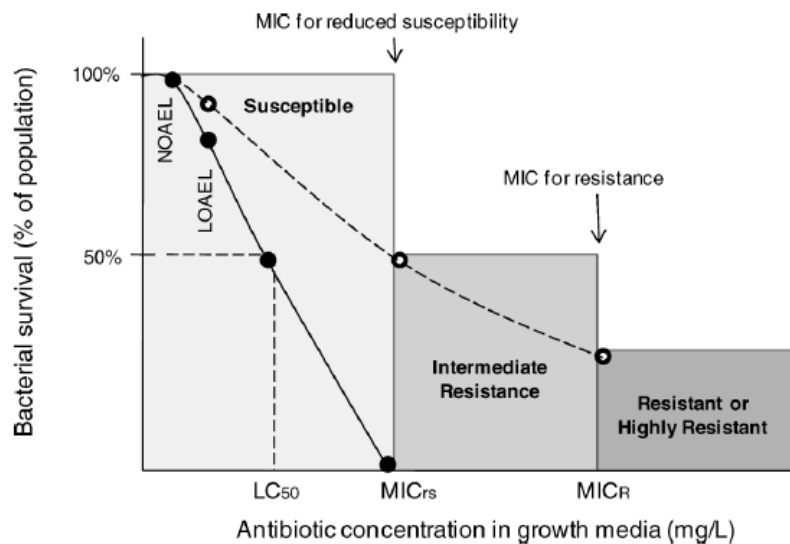


Figure 5: Hypothetical Antibiotic Dose Relationship for Normal and Resistant Bacteria (Nagulapally et al., 2008)

The figure shows that the mortality rate of bacteria increases as the antibiotic concentration increases. The concentration that produces a 50% reduction in the population of bacteria is known as the lethal concentration for 50% mortality, or  $LC_{50}$ . No observed adverse effect level (NOAEL), lowest observed adverse effect level (LOAEL), and  $LC_{50}$  depend on the types of

bacteria and antibiotics present in the wastewater and the environmental conditions. Matrix chemistry also has a role because it deals with mixtures of bacteria and antibiotics and the different chemical reactions that could happen in wastewater under varying environmental conditions. Bacteria that survive higher antibiotic concentrations are considered to be resistant and have reduced susceptibility to the drug.

Minimum inhibitory concentration (MIC) is another factor used to describe bacterial vulnerability to antibiotics. Figure 5 shows that the MIC for resistance ( $MIC_R$ ) is the lowest in vitro concentration in which an antibiotic completely hinders the growth of bacteria. The MIC for reduced susceptibility ( $MIC_{rs}$ ) is the concentration at which bacteria can survive and indicates the development of intermediate resistance. Ultimately, organisms that survive between the two MIC points develop an intermediate resistance and bacteria that exist at higher concentrations have a greater resistance to the antibiotic (Nagulapally et al., 2008).

Nagulapally et al. (2008) evaluated the occurrence of antibacterial-resistant bacteria in aqueous samples obtained from a municipal WWTP. Samples were collected from the influent, clarifier effluent, and the disinfected effluent. Fecal coliforms like *E. coli*, and enterococci were measured for exhibiting resistance to CIP and two other drugs. Intermediate and high resistance was observed for CIP, which has a  $MIC_{rs}$  of 1 mg/L and a  $MIC_R$  of 4mg/L. Significant intermediate resistance was observed in fecal coliforms, with approximately 3.5% of the total fecal coliforms and 52% of the enterococci in the influent showing reduced susceptibility to CIP. *E.coli* was completely deactivated at 1 mg/L CIP in the winter and some intermediate resistance was observed under the same concentration during the spring.

Manaia et al. (2010) assessed the potential of domestic wastewater treatment plants (WWTP) contributing to the distribution of CIP-resistant bacteria. Nutrient rich environments like sewage sludge and wastewater provide a favorable environment for horizontal gene transfer which enables a way for plasmids and transposons to encode antibiotic resistance. Therefore, wastewater treatment plants are considered “hot spots” for antibiotic resistance spreading because high populations of antibiotic resistant bacteria are mixed together. Wastewater containing antibiotics including CIP is discharged at many locations that include hospital and industrial effluents as well as urban and domestic areas. In order to decrease the amount of pathogens discharged a disinfection process must be implemented within the treatment plant. Though, this disinfection process must be carefully analyzed because there is evidence that some

treatments promote resistant bacteria. For example, long hydraulic retention times (HRT) for the disinfection process have higher bacterial removal rates but horizontal gene transfer is more favored while lower HRT allows for greater amounts of bacteria discharged in the treated effluent. The study showed that weather conditions for the wastewater entering the plant did not affect the bacterial load released from the plant, but that larger wastewater treatment plants discharged higher densities of bacteria compared to smaller plants. It is determined that WWTPs supply antibiotic resistant bacteria to the environment and a treatment step eliminating the antibiotic from the water prior to discharge must be closely analyzed.

### **2.2.3 Environmental Risks of CIP**

Antibiotics are biologically active molecules that are designed specifically for controlling pathogenic bacteria in animals and humans, but there is very little information on their ecotoxicology. Most of the antibiotics that are administered to humans and animals are excreted into wastewater where they enter WWTPs. If they are not completely mineralized in the WWTP then they are released into surface waters and sludge (Halling – Sørensen et al., 2000). Antibiotic sorption onto sewage sludge has been shown to be a favorable removal pathway from wastewater streams. Sewage sludge has been regularly used as topsoil fertilizer which represents another possible route for pharmaceuticals to enter the environment (Golet et al., 2003). Large volumes of pharmaceuticals are also released into surface waters yearround via WWTP effluents and untreated human and livestock sewage. Even though large volumes are released daily into surface water, the effects of pharmaceuticals on the aquatic ecosystem remains largely unknown, thus there are many concerns revolving around the organisms that inhabit the surface waters receiving the sewage (Richards et al., 2003).

Halling – Sørensen et al. (2000) assessed the effects of CIP and two other antibiotics on the aquatic environment by investigating the toxicity of the 3 antibiotics towards sludge bacteria, a green alga, a cyanobacterium, a crustacean and a fish. Results showed that CIP was highly toxic to the cyanobacterium, *Microcystis aeruginosa*. A risk characterization was performed by calculating the predicted environmental concentration and the predicted no effects concentration and then finding the ratio between the two. A ratio less than one indicated that, with the present pattern of use, no environmental risk is expected. Of the three antibiotics, CIP had a ratio greater than one for the present usage in Europe.

Richards et al. (2003) exposed outdoor microcosms to a mixture of ibuprofen, fluoxetine, and CIP at concentrations of 6, 8, and 10 µg/L (low treatment), 60, 80, and 100 µg/L (medium treatment), and 600, 800, and 1000 µg/L (high treatment) for 35 days. Low treatment showed few responses, but medium and high treatment had observed effects. Fish died under medium treatment in less than 35 days and under high treatment in less than 4 days. Phytoplankton increased in abundance and decreased in diversity in high treatment and medium and low treatment showed consistent trends. Zooplankton showed similar trends for the three treatments. The present data does not show that the 3 antibiotics are individually causing adverse effects in surface waters, but there are questions that remain about the additive responses from mixtures.

Robinson et al. (2004) performed toxicity tests with seven FQs, including CIP, on five aquatic organisms, *Pseudokirchneriella subcapitata* (formerly *Selenastrum capricornutum*) and *Microcystis aeruginosa*, algal species from two divisions (Chlorophyceae and Cyanophyceae), *Lemna minor* (duckweed), *Daphnia magna* (waterflea), and *Pimephales promelas* (fathead minnow). The results showed that tests with the crustacean and fathead minnow showed limited toxicity with no effects at or near concentrations of 10 mg/L, but the fish dry weights obtained with the CIP treatment were significantly higher than in the control fish. The average environmental concentration of the seven FQs was 1µg/L which was based on previous surface water concentrations reported in environmental journals. At this concentration, only the algal species, *M. aeruginosa*, may be at risk in surface water.

## **2.3 Potential Treatment Methods**

### **2.3.1 Adsorption**

Among many applications, adsorption is often used to remove contaminants from water. Adsorption is defined as the process by which contaminant molecules accumulate on the surface of a solid at the interface between the two phases present. The contaminant adsorbed is referred to as the adsorbate and the solid is referred to as the adsorbent.

There are two major methods of adsorption; chemisorption and physisorption. Chemisorption can only occur in monolayer due to the necessity for a specific adsorption site for each bond formed. This accumulation occurs through valence bonds that cause a drastic shift of electron density resulting in covalent or ionic bonds. However, physisorption can accumulate in multiple layers. The layers are formed through weak intermolecular van der Waals forces which

cause an almost negligible shift in electron density and therefore do not require a specific site on the adsorbent. In this process, there are no new chemical species introduced; the contaminant is simply removed from the water (Letterman, 1999).

The physisorption process occurs in four major steps; bulk solution transport, external (film) resistance to transport, internal (pore) transport, and adsorption (Letterman, 1999). Bulk solution transport is the movement of the contaminant from the bulk water solution to the thin layer around the adsorbent particles. Once the contaminant has come in contact with the boundary layer surrounding the adsorbent particle, external resistance to transport occurs while the contaminant is “transported by molecular diffusion through the hydrodynamic boundary layer” (Letterman, 1999). Pore transport then occurs in order to pass the contaminant from the hydrodynamic boundary layer through the pores to the vacant adsorption sites along the surface. At this point, intermolecular bonds are rapidly formed between the contaminant and the adsorbate and the contaminant is successfully removed from water. The adsorbent will continue to accumulate on the surface until saturation is reached. The process will then be at equilibrium and the rate of the reverse process of desorption will be equal to the rate of adsorption and no further accumulation will occur (Roque-Malherbe, 2007).

### **Factors Affecting Adsorptivity**

The bond types as well as temperature, pH, and properties of the adsorbate and adsorbent all have an effect on the amount of contaminant that will be adsorbed by the surface. The bonds formed at the surface include van der Waals, dipole-dipole, and hydrogen-bonding, which are listed with increasing strength. Typically, the temperature and pH are set as operating conditions and remained relatively constant. The properties of the adsorbate that must be taken into consideration include the pKa, solubility in water, concentration in water, size, and geometric structure. It is important for adsorption effectiveness that the adsorbate has a higher affinity for the adsorbent than for water. Therefore, a higher solubility will most likely result in a lower adsorption rate (Roque-Malherbe, 2007).

The properties of the chosen adsorbents that will affect removal of ciprofloxacin include the specific surface area, pore structure, polarity, micropore volume, and pore size distribution. A higher specific surface area, normally measured in  $\text{m}^2/\text{g}$ , is desired to increase the capacity for adsorption. Although it is necessary to use an adsorbent with pores large enough to allow for

transport by the contaminant, the smallest adequate pores will allow for a higher surface area and therefore more available sites for adsorption. All other parameters for adsorbents must be designed for compatibility with CIP (Yang, 2003).

### **Activated Carbon**

Silica gel, porous alumina, silica-alumina, and zeolites are all common choices for adsorbents; however the most common adsorbent is activated carbon. It is often used because it has a high specific surface area (300-400 m<sup>2</sup>/g), which increases the number of sites available for pentagonal, hexagonal, and heptagonal carbon rings. Activated carbon has a non-polar surface, which makes it an ideal adsorbent for non-polar contaminants. Only van der Waals forces are available for bonding, which causes the adsorption process to be highly reversible (Yang, 2003).

### **Isotherms**

Isotherms are generated in order to characterize the relationship between the contaminant being adsorbed and the adsorbent. It is produced using equilibrium data at a constant temperature where the amount of contaminant adsorbed per unit of adsorbate, or loading, is plotted against the equilibrium concentration of contaminant remaining in solution. The data can then be fit to a range of isotherm models to determine the most appropriate equation to describe the relationship. The Langmuir and Freundlich models are most commonly used (Yang, 2003).

### **Freundlich Model**

The Freundlich model is expressed as a power function shown in Equation 1.

$$q = K_f C_e^{1/n} \quad (1)$$

Where

q = loading, or the mass of contaminant adsorbed per mass of adsorbent (mg/g)

C<sub>e</sub> = equilibrium concentration (mg/L)

K<sub>f</sub> = Freundlich coefficient

n = empirical coefficient

Using this relationship, a plot of the natural log of the loading vs. the natural log of the equilibrium concentration should yield a linear line with a slope of  $1/n$  and an intercept of  $\ln K_f$ . The parameter  $K_f$  is related to the capacity of the adsorbent for the contaminant and  $1/n$  represents the strength of adsorption (Letterman, 1999).

### Langmuir Model

The Langmuir model is used to represent single-layer adsorption and can only be used under the following assumptions:

1. Each molecule is only adsorbed to one specific site that does not contain any other molecules.
2. The sites are all equivalent in energy and the molecules adsorbed will only interact with the site they adsorb to, not the sites adjacent to them.
3. The system is at constant temperature.
4. The adsorption occurs only in one layer.

In order to fit a Langmuir model to equilibrium data, the equilibrium assumption that the rate of adsorption is equal to the rate of desorption is applied. The rate of adsorption is shown in Equation 2 and the rate of desorption is shown in Equation 3. These are set equal to each other to represent a state of equilibrium as shown in Equation 4 (Douglas, 1985).

$$\text{Rate} = k_a C_e (1-\theta) \quad (2) \text{ (rate of adsorption)}$$

$$\text{Rate} = k_d \theta \quad (3) \text{ (rate of desorption)}$$

$$k_a C_e (1-\theta) = k_d \theta \quad (4)$$

where

$k_a$  = adsorption rate constant

$k_d$  = desorption rate constant

$\theta$  = fraction of adsorbate surface covered,  $q/q_m$

$q_m$  = total number of sites per unit weight of adsorbent

After rearranging and setting  $k_a/k_d$  to a single constant,  $b$ , and  $\theta$  to  $q/q_m$  the result is Equation 5:

$$\frac{1}{q} = \frac{1}{q_m} + \frac{1}{bqC} \quad (5)$$

Therefore, a plot of  $1/q_{vs}1/C$  can be generated to obtain a straight line with slope of  $\frac{1}{bq_m}$  and an intercept of  $\frac{1}{q_m}$ . (Douglas, 1985; Roque-Malherbe, 2007)

### **Recent Studies**

Many recent studies have been conducted on the removal of pharmaceuticals using adsorption to soils, clay, activated carbon, and other adsorbents. CIP in particular has been successfully removed from water using adsorption to montmorillonite clay, aluminum hydroxides, iron hydroxides, and goethite; however there is little information about its ability to adsorb to activated carbon.

Recent research has demonstrated a strong effect of solution pH on the amount of CIP adsorbed. Results found that adsorption to aluminum hydroxides, iron hydroxides, and goethite, neutral pH was most effective (Huang and Zhang, 2006; Karthikeyan and Gu, 2005). It was similarly concluded that keeping solution pH below the second pKa of CIP yielded the most success with montmorillonite clay as the adsorbent (Li et al. 2010). All experiments also showed a strong correlation to the Langmuir adsorption model. In addition, mechanisms for adsorption to goethite were studied. It was concluded that the adsorption process was accompanied by slow oxidation by goethite and that the carboxylic group in CIP was essential for adsorption while the piperazine ring remained susceptible to oxidation (Huang and Zhang, 2006). Although this information is useful for determining operating conditions for activated carbon adsorption, the surface chemistry will vary from adsorbents studied and therefore must be looked at as a completely separate set of experiments.

### **2.3.2 Advanced Oxidation Treatments (AOPs)**

#### **Ultraviolet Degradation**

Ultraviolet degradation for emerging contaminants, such as CIP, has been a progressively implemented technique in the United States and Europe. This system uses UV light, occasionally in the presence of additional chemicals, to perform radiation, photolysis or oxidation. There are several types of UV systems which utilize different types of lamps and radiation wavelengths. UV treatment is often used in conjunction with other conditions and treatment methods to improve the amount and rate of degradation.



The types of UV treatment systems mainly differ due to the lamps used to produce radiation. The first uses a low pressure mercury vapor lamp which produces quasi-monochromatic UV light at 254 nm. The second system uses either medium pressure UV lamps or medium pressure mercury lamps, which produce a polychromatic output ranging from 200nm to visible and infrared energy, upwards of 350nm. The low pressure lamps tend to be more efficient; however the medium pressure lamps have a higher UV-C intensity per lamp, which means fewer are needed (Pereira et al., 2007). In each system, the UV light and exposure time is measured in  $\mu\text{W}\cdot\text{s}/\text{cm}^2$ . When developing a radiation profile, variables include water quality, lamp type, and the transmittance and dimension of the quartz sleeve containing the batch of water.

UV treatment can also be enhanced with the addition of a photocatalyst to the solution prior to treatment, as well as the adjustment of pH before treatment. In some studies, varying pH had a great effect on the success and degradation rate of material, especially CIP. When studied in solution and in a mixture, CIP degraded more completely when treated at pH 7 with UV (Avisar et al., 2010, Doorslear et al., 2010). Additionally, Avisar et al. (2009) recommended using UV treatment in conjunction with a biological filter or pre-filtering to remove large particles.

### **Photolytic Treatment**

When used alone, UV treatment causes photolysis to occur within the sample. In photolysis, the chemical species undergoes a chemical change as an effect of absorbing photons. This creates an “excited state, where it is more likely to transform” (Avisar et al., 2010). Chemicals can usually only undergo photolysis under the influence of UV if it is absorbing at wavelengths lower than 300nm. Figure 6 shows the mechanism for UV degradation of a FQ.

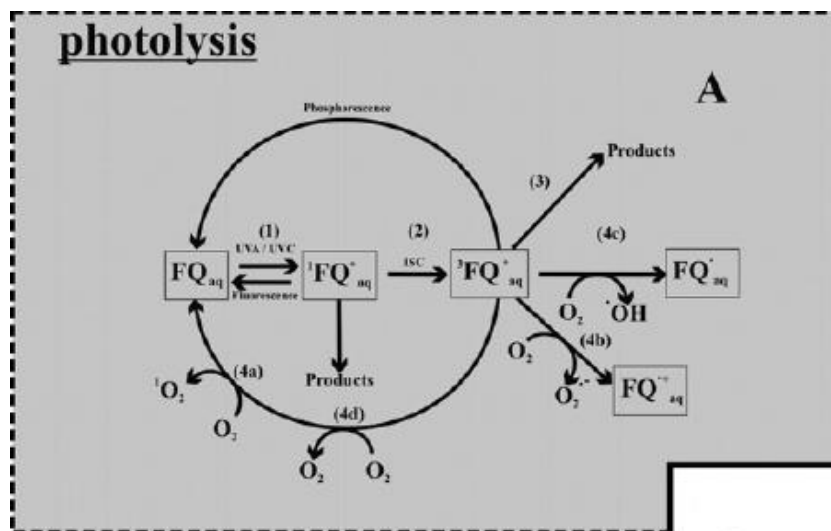
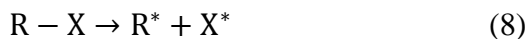
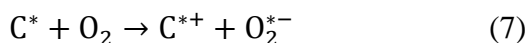


Figure 6: FQ Mechanism of UV Degradation During Photolysis (Doorslear et al., 2010.)

Photolysis is able to destroy components in water; however it does not completely degrade them. In the study performed by Pereira et al., it was found that CIP had the highest absorption rate of UV light,  $3000 \text{ M}^{-1}\text{cm}^{-1}$ , between the range of 250-290nm, with a peak at 270nm. In this range, the medium pressure lamps are more effective than the low pressure; however both types are still able to produce radiation that CIP will absorb. The study showed that MP-UV photolysis and UV/H<sub>2</sub>O<sub>2</sub> yielded a very small fluence-based rate constant of  $0.001 \text{ cm}^2/\text{mJ}$  for CIP, suggesting that it is not the most easily effected water contaminant. Equations 6 through 9 illustrate the UV induced photolytic reaction mechanism:



Equations 6-9: UV Induced Photolytic Reaction Mechanism (Legrini et al., 1999)

In this series of reactions, UV light causes electron transfer from an excited state ion to ground state oxygen (Eqs. 6 and 7). Then hydrolysis or recombination of radical ions form radicals which react with oxygen molecules (Eqs. 8 and 9) (Legrini et al, 1993). In particular, UV light hits FQ molecules and excites them to its singlet state. Then through intersystem crossing, a singlet state FQ can go to its triplet state. The singlet and triplet state of a molecule

are the energy levels with the highest probability to undergo photo-induced chemical reaction. FQ oxidation is mainly dependent on the FQ triplet state and two mechanisms of triplet state FQ degradation can result: direct oxidation with the formation of degradation products as a result of defluorination, decarboxylation, and side chain degradation (Doorslaer et al., 2010).

### Photocatalytic Treatment

Photocatalytic oxidation occurs when UV treatment is used with the addition of a photocatalyst in solution, such as hydrogen peroxide or titanium dioxide. Advanced oxidation produces highly reactive and non-selective hydroxyl radicals that increase the rate of degradation. This method can be very effective in treatment of several water contaminants (Pereira et al., 2007). The efficiency of photocatalytic treatment depends on the water quality, compound type, and UV dosage (U.S. Department of the Interior Bureau of Reclamation, 2009). Photocatalytic oxidation by addition of H<sub>2</sub>O<sub>2</sub> is the result of the CIP being attacked by both UV photons and the hydroxyl radicals made from the cleavage of the H<sub>2</sub>O<sub>2</sub> molecule. This reaction not only results in the decomposition of organic compounds, but also the regeneration of additional H<sub>2</sub>O<sub>2</sub> molecules (Elkanzi, 1999). Equations 10 through 15 below illustrate the reactions that occur in photocatalytic oxidation and degradation of CIP with UV/H<sub>2</sub>O<sub>2</sub>.



**Equations 10-15: H<sub>2</sub>O<sub>2</sub> Photolytic Oxidation Reaction Mechanism (Legrini et al., 1999).**

In order to enhance UV transmittance, remove total organic carbon (TOC) and keep costs at a feasible level, GAC is generally implemented for pretreatment. Two major issues that arise from implementing GAC are inorganic material that is not removed acts as a scavenger for the hydroxyl radicals, and high water hardness fouls the UV tubes, which increases the need for frequent cleaning. Despite its high cost, photocatalytic degradation is one of the most effective

technologies for removing emerging contaminants (U.S. Department of the Interior Bureau of Reclamation, 2009).

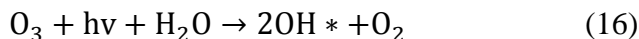
### 2.3.3 Additional AOPs

#### Ozonation

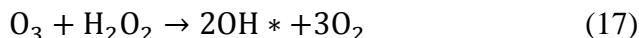
Ozone, O<sub>3</sub>, is the triatomic form of oxygen and is a very unstable gas, readily degrading back to oxygen. During the transition to oxygen, free oxygen radicals are formed that are highly reactive and able to only exist for milliseconds. Ozone is a colorless gas and has an odor similar to the smell of air after a thunderstorm.

In water, ozone decomposes and forms free radicals such as HO<sub>2</sub>\* and OH\*. The formation of the hydroxyl radical (OH\*) is sought for in water treatment processes because they are an extremely reactive species that can attack almost any organic substance (Glaze, 1986). Accelerating the ozone decomposition rate increases the hydroxyl radical concentration, and thus the oxidation rate. Generally, ozone reacts with organics found in water through direct molecular and indirect radical chain type reactions depending on the pH and composition of water. At acidic pHs, molecular ozone is the major oxidant, but faster hydroxyl radical oxidation becomes more favored at pH greater than 7. The oxidation potential of hydroxyl radicals is much higher than ozone molecules, thus direct oxidation is slower than radical oxidation and can result in incomplete oxidation of organic compounds (Balcioglu, 2003). One of the most common processes for increasing the rate of ozone decomposition is by adding hydrogen peroxide, H<sub>2</sub>O<sub>2</sub> to ozonated water (EPA, 1999). This process is commonly referred to as peroxone.

The main chemical reaction of the photolysis of ozone is:



With the addition of hydrogen peroxide, the main chemical reaction yields:



Ozonation of wastewater is a process in which dry, clean air is passed through a high voltage electric discharge which creates variable ozone concentrations. Raw water is then passed through a venturi throat which creates a vacuum and pulls the ozone gas into the water where the air is bubbled through the water. In situations where ozone reacts with metals to create insoluble metal oxides, post filtration is required.

There are several advantages and disadvantages for using ozone as a treatment method.

The advantages include:

- ◆ effectiveness over a wide pH range
- ◆ high oxidizing power with a short reaction time
- ◆ can eliminate a variety of inorganic, organic and microbiological problems
- ◆ reduces oxygen demanding matter, turbidity, and surfactants

And the disadvantages are:

- ◆ high capital costs and high electric consumption
- ◆ the by-products are still being evaluated for their potential in being carcinogenic
- ◆ not effective at removing dissolved minerals and salts

Additionally, there have been several recent studies that have looked at the effects of ozone on CIP in deionized water and hospital effluent samples.

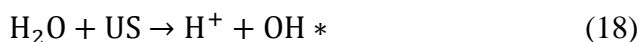
De Witte et al. (2009) studied the effects of ozonation on CIP in deionized water when varying inlet concentration of ozone, CIP concentration, temperature, pH, and H<sub>2</sub>O<sub>2</sub> concentration. From HPLC-MS analysis, desethylene CIP was found as one of the degradation products. Desethylene CIP formation was dependent on pH, with pH 10 yielding the highest concentrations. Fast CIP ozonation occurred at pH 3 which was suggested to happen because other radical species besides hydroxyl radicals may form at the acidic pH.

Vasconcelos et al. (2009) recognized that few studies have investigated degradation of different pharmaceuticals, including CIP, with “real samples”, therefore their study examined the degradation of CIP in hospital effluent by photo-induced oxidation, heterogeneous photocatalysis, ozonation, and peroxone experiments. CIP was detected in the effluent samples by liquid chromatography and fluorescence detection (LC-FLD). Photo-induced oxidation was the slowest in degrading CIP, and both heterogeneous photocatalysis and peroxone led to almost complete degradation after 60 minutes. Ozonation showed the best performance overall with CIP completely degrading after 30 minutes which was unexpected because the latter two processes generate more hydroxyl radicals. Vasconcelos et al. concluded that the byproducts formed during the processes were very similar and that the byproducts could be derived from the oxidation of the piperazine group.

De Witte et al. (2010) also studied the ozonation of CIP in hospital WWTP effluent. The article focused on parent compound degradation, degradation product identification and residual antibacterial activity. First, CIP sorption onto a suspended solid as a function of temperature and pH was conducted for ozone efficiency. The results showed the temperature does not affect sorption, but sorption was most effective at pH 7 compared to pH 3 and 10. CIP ozonation was slowest at pH 7 with greater half-life times compared to pH 3 and 10. Adding H<sub>2</sub>O<sub>2</sub> increased the half-life times even more which most likely can be justified by both H<sub>2</sub>O<sub>2</sub> and radical species competing for ozone. Desethylene CIP was detected again and its formation was dependent on pH as before with ozonation in deionized water.

### **Sonolysis**

Recent advances in the ultrasonic field have enabled the introduction of ultrasonic disintegration techniques which can reduce the amount of contaminants found in municipal sewage sludge. The expected effect is sonolysis, or cell lysis, in which sludge microorganisms are destroyed and the subsequent release of dead cells into the sludge liquid that can increase the COD of the substances in the liquid (Zielewicz, 2008). The mechanism of sonolysis is based on cavitation, which is the rapid formation, growth, and sudden collapse of bubbles in liquids from sound waves (kHz - MHz) applied to a liquid medium convert sound energy into heat for chemical reaction.



Cavitation has been widely explained by the “hot spot” theory which says that when cavitation bubbles implode, temperatures as high as 5200K and pressures higher than 100MPa are reached inside the collapsing cavity. There are two possible degradation routes; the contaminant can undergo thermal degradation inside and at the interfacial region of the cavity and free radicals (predominately OH\*) are formed from the thermolysis of water and react with the contaminant at the interfacial surface or in the bulk solution (De Bel et al., 2009).

De Bel et al. (2009) studied the effects of sonolysis at 520 kHz and 92 W/L for the degradation of CIP. After 120 min, a pH 7 solution of CIP degraded by 57%. pH proved to be an important parameter because the pseudo first order degradation constant increased fourfold when comparing treatment at pH 7 and pH 10 to treatment at pH 3. This effect is explained by the degree of protonation of the CIP molecule at each pH. The BOD/COD ratio of the solutions,

which is a measure of their biodegradability, increased for all three pH values and pH 3 was considered readily biodegradable because it had a ratio greater than 0.4. The antibiotic activity against *E. coli* and *B. coagulans* of the treated solutions was reduced after sonolysis with the highest decrease at pH 3, but the ecotoxicity of the solutions to the alga *Pseudokirchneriella subcapitata* increased 3- to 10-fold after 20 minutes of treatment which suggests formation of toxic degradation products. Further treatment slowly reduced the toxicity.

## **2.4 Summary**

The occurrence of CIP in aquatic ecosystems is a cause for concern because of the possibility for bacterial resistant organisms in sewage sludge. The effects on organisms in aquatic ecosystems and CIP adsorption onto sediments in various water bodies are also environmental risks that have been identified, but not thoroughly researched. AOPs and adsorption applications are known treatment methods for degrading CIP in water and wastewater effluents, but optimal conditions for each treatment process have yet to be found due to inconsistencies in the findings.

## **Chapter 3: Methodology**

### **3.1 Sample Preparation**

Solutions of known initial concentrations of CIP received from LKT Laboratories in Barnstead E Pure Water (ROpure ST Reverse Osmosis/tank system) were created for each experimental treatment. Predetermined masses of CIP were weighed using a Mettler Toledo (AB104-S) scale and added to E-Pure water. The solutions were stirred thoroughly with a magnetic stirrer for a minimum of 20 minutes, until a well-mixed solution was achieved with all CIP dissolved. Samples were adjusted to pH 3, pH 7, or pH 10 by the drop-wise addition of NaOH or HCl and the use of an Accumet Basic AB 15 pH meter (Fisher Scientific).

### **3.2 Measuring Sample Absorbance**

Analysis of the samples of CIP solutions was completed before and after treatment to determine the amount of CIP removed during each trial. To complete analysis of each sample, a Varian-Cary 50 Scan UV - visible spectrophotometer was used with Plastibrand UV-cuvette micro (12.5x12.5x45mm) cuvettes to measure the absorbance. The spectrophotometer was operated at a wavelength of 280 nm.

### **3.3 Ciprofloxacin Concentration Standard Curves with Detection Limit**

In order to determine the unknown concentration of treated samples, standard concentration curves at pH 3, pH 7, and pH 10 were created with samples of solutions at known concentrations. Solutions of ten known concentrations, ranging from 0.001 mg/L to 20 mg/L of CIP in water, at each pH were analyzed by the Varian-Cary 50 Scan UV - visible spectrophotometer to measure the absorbance. The correlation between the known concentration of the sample and the measured absorbance was used to develop standard concentration curves at each of the three pH levels. In addition, samples of a known concentration of CIP were compared to blank samples using a T-test in excel to determine the detection limit below which there was no longer a statistical difference between a blank sample and one containing CIP. The excel sheet for this analysis is shown in Appendix C.



### 3.4 Ultraviolet Treatment

Ultraviolet treatment was performed in a lab scale batch reactor as shown in Figure 7, a glass tube apparatus, which held a small UV lamp surrounded by approximately 15 mL of solution. Both a Pen-Ray 5.5 watt Lamp (ACE No. 12132-08), a low pressure mercury vapor lamp producing UV light at 254 nm, and a Spectronics Corporation Specroline 36-380 Long Wave Pencil Lamp, a medium pressure UV lamp producing UV light at 365nm, were used for treatment. Initial experiments were conducted for a specified exposure time at which any additional time would result in a negligible difference in CIP concentration. In addition, experiments were run at smaller time intervals to closely examine the effect of time on the treatment. The time trials were conducted with solutions of an initial concentration of 20 mg/L CIP in water at pH 3, pH 7, or pH 10. Additionally, hydrogen peroxide was added to solutions before UV treatment.

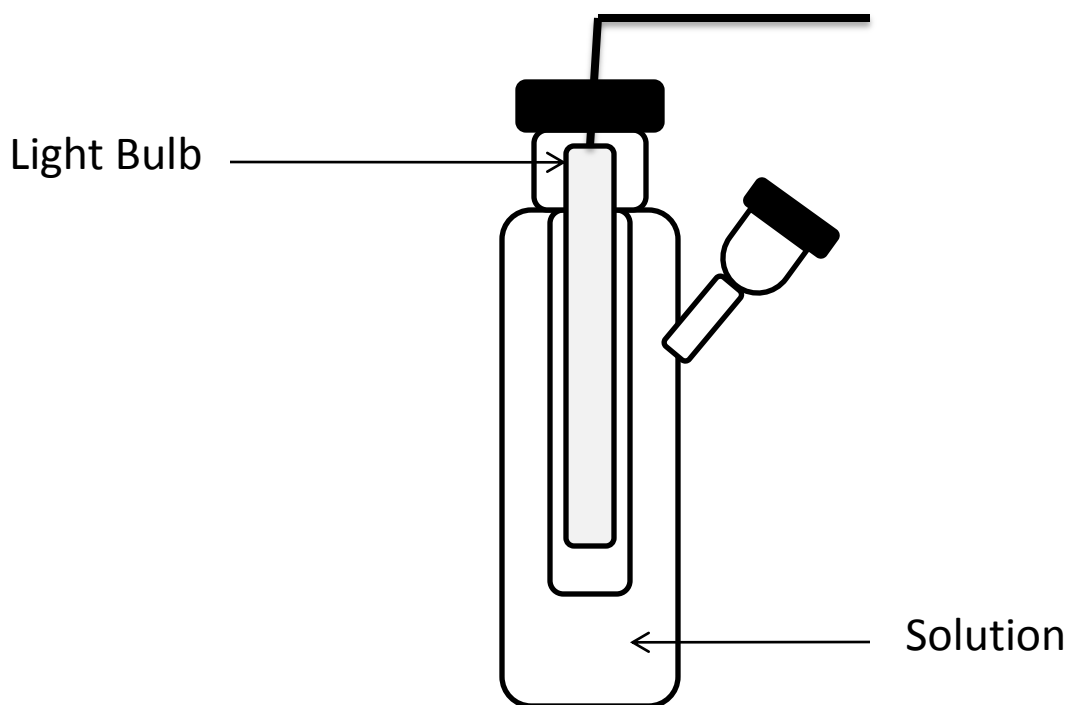


Figure 7: UV Treatment Glass Tube and Light Apparatus

#### 3.4.1 UV Photolysis: 75 minute exposure time

UV photolysis experiments were conducted by exposing the samples of solution at each pH for 75 minutes to the UV light to ensure the maximum degradation of CIP. The experiments were conducted at both UV wavelengths to determine which wavelength was more effective in

removing the CIP from solution. After the samples were treated, the pH was measured again and adjusted back to the initial pH. The samples were then analyzed by the spectrophotometer to determine the final absorbance. This value was used in correlation with the previously constructed concentration standard curves in respect to final pH.

### **3.4.2 UV Time Trials**

Time trials were conducted to determine the reaction kinetics, or rate of reaction and degradation of CIP, during UV treatment. Treatment was performed at UV light exposure time intervals of 2, 4, 6, 10, 20, 30, 60, and 75 minutes, for the solutions at each pH. After each experimental run had been completed, the pH of each sample was adjusted to its original pH and the sample was analyzed by the spectrophotometer to determine the final absorbance and related to a new concentration.

### **3.4.3 Ultraviolet Treatment with Addition of Hydrogen Peroxide**

Further UV treatment was conducted with the addition of hydrogen peroxide to aid in the degradation process. UV treatment with the addition of hydrogen peroxide (UV/H<sub>2</sub>O<sub>2</sub>) experiments were done by adding hydrogen peroxide to the solution before implementing the same treatment method described above. For the 45 minute trials, hydrogen peroxide was added to 20 mg/L CIP solutions based on molar ratio. Solutions were created of 100:1, 50:1, 10:1, 5:1, and 1:1 molar ratios of hydrogen peroxide to CIP. The solutions were exposed to UV light for 45 minutes. After each experimental run had been completed, the samples were analyzed by the spectrophotometer to determine the final absorbance and related to a new concentration. The molar ratio of 50:1 hydrogen peroxide to CIP was the most successful ratio for removing the greatest percent of CIP, and was therefore used to conduct additional time trials. The time trials were conducted at intervals of 2, 4, 6, 10, 20, 30, and 60 minutes at each pH. After each experimental run was completed, the samples were analyzed by the spectrophotometer to determine the final absorbance and related to a new concentration.

### **3.5 Adsorption Treatment**

The adsorption treatment experiments were performed to analyze the effect of the type of adsorbent and time required for removal. The adsorbents tested were F-600 and F-200GACs,

which were obtained from Calgon Carbon Corporation. Adsorption was conducted first to equilibrium, and then in time trials. Equilibrium occurs when the rate of adsorption equals the rate of desorption and no further accumulation of CIP on the surface occurs. For each experiment, the desired mass of activated carbon was weighed and added to 42 mL glass vials. Solution was added to the vials and securely capped before being placed into a rotisserie mixer to maintain uniform motion, mixing, and adsorption. After treatment, each sample was removed from the mixer and centrifuged in the Eppendorf Centrifuge 5804 for 20 minutes at 2680 rpm, which was the highest speed that the vials could safely withstand. The solution was then pipetted into glass beakers for analysis.

### **3.5.1 Adsorption Equilibrium Trials**

The equilibrium trials were conducted to 48 hours of contact time to ensure the maximum adsorption of CIP. In the equilibrium trials, the initial concentration of CIP solution, type of adsorbent, and pH were varied. The initial concentrations of CIP in solution were 100, 150, 200, 250, and 300 mg/L. The solutions were added to vials containing 0.1 g of F-600 GAC or 0.1 g of F-200 GAC. After the samples were treated, centrifuged, and removed from the vials, the pH was measured again and adjusted back to the initial pH. The samples were then analyzed by the spectrophotometer to determine the final absorbance. This value was used in correlation with the previously constructed concentration standard curves in respect to final pH.

### **3.5.2 Adsorption Time Trials – Kinetics**

The time trials were conducted with solutions of an initial concentration of 100 mg/L CIP added to vials containing 0.1 g of F-600 GAC or 0.1 g of F-200 GAC. Time trials were conducted at intervals of 2, 4, 8, 12, 24, and 48 hours at pH 3, pH 7, and pH 10. After each experimental run had been completed, the samples were centrifuged and removed from the vials. The pH was measured again and adjusted back to the initial pH. The samples were analyzed by the spectrophotometer to determine the final absorbance and related to a new concentration.

## Chapter 4: Results and Discussion

The objective of this study was to obtain data for the removal of CIP from water using adsorption to activated carbon and the degradation of CIP by UV and UV/H<sub>2</sub>O<sub>2</sub> at pH 3, 7, and 10. The data were analyzed to determine the relative effectiveness of each removal method in order to make recommendations for treatment as well as future research.

### 4.1 Calibration Curves

A separate calibration curve was established at each tested pH using the UV spectrometer at wavelength 280 nm to use as a method of detection after treatment. The three curves are plotted below in Figure 8.

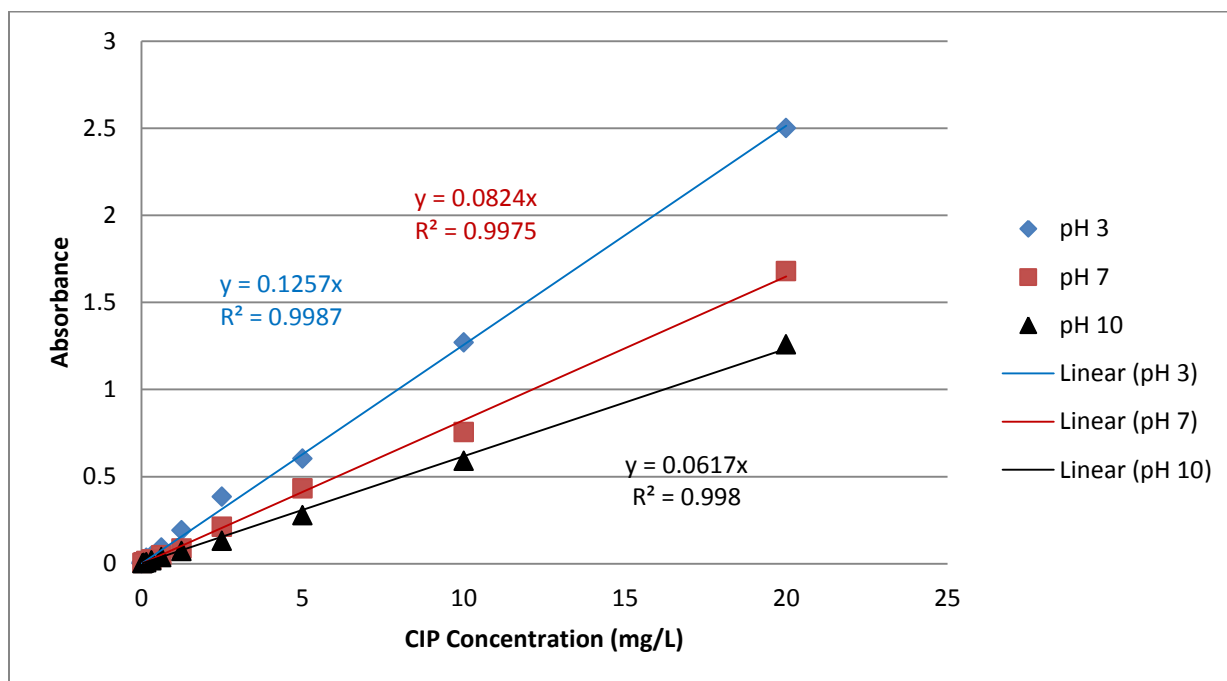


Figure 8: Calibration curves for UV spectrometer at 280 nm

All curves were considered an accurate form of detection below concentrations of 20 mg/L, with R<sup>2</sup> values above 0.997. The difference in slope at each pH can most likely be attributed to the change in speciation after passing through the two pK<sub>a</sub> values. At pH 3, the cationic form of CIP is dominant due to protonation of the amine group in the piperazine moiety. At pH 7, CIP loses a hydrogen atom off the nitrogen in the piperazine moiety thus establishing a

balance of charges on the molecule. This balance is characteristic of the zwitterionic form for CIP. At pH 10, after passing the second pKa, a proton is lost from the carboxylic group and the anionic form of CIP is dominant in solution (Wu et al., 2010).

## 4.2 UV Degradation

### 4.2.1 Determination of Effective UV Wavelength

Initial UV photolysis experiments were conducted at each pH for 75 minutes with both UV bulbs available in order to determine which wavelength would be most successful at degrading CIP. Results are shown in Table 1. It was determined that 60 minutes was required to obtain an almost minimum concentration of CIP in solution. Experiments were run for an additional 15 minutes to ensure that there was not a noticeable decrease in concentration with increasing exposure time.

Table 1: UV wavelength comparison

| Wavelength (nm) | Total Time (min) | pH | % Decrease |
|-----------------|------------------|----|------------|
| 365             | 75               | 3  | 32.8       |
|                 | 75               | 7  | 26         |
|                 | 75               | 10 | 7.2        |
| 254             | 75               | 3  | 97.2       |
|                 | 75               | 7  | 94.4       |
|                 | 75               | 10 | 90.2       |

Table 1 shows that the shorter 254nm wavelength was significantly more effective at degrading CIP in water than the longer 365 nm wavelength and therefore it was used for all experiments with UV and UV/H<sub>2</sub>O<sub>2</sub>. It is also important to note that with both wavelengths, the percent degradation of CIP from water decreases with increasing pH.

### 4.2.2 UV Photolysis

UV photolysis kinetics trials were conducted with a constant initial concentration of 20 mg/L from time zero to 75 minutes at each pH. This was done in order to establish UV photolysis reaction rate laws and make comparisons of rates as well as overall degradation for each pH. The final concentration of CIP remaining after 75 minutes was used for final percent degradation values shown above in Table 1. Figure 9 shows the kinetics data obtained at each

pH, and demonstrated that 60 minutes was clearly adequate time to achieve close to maximum degradation.

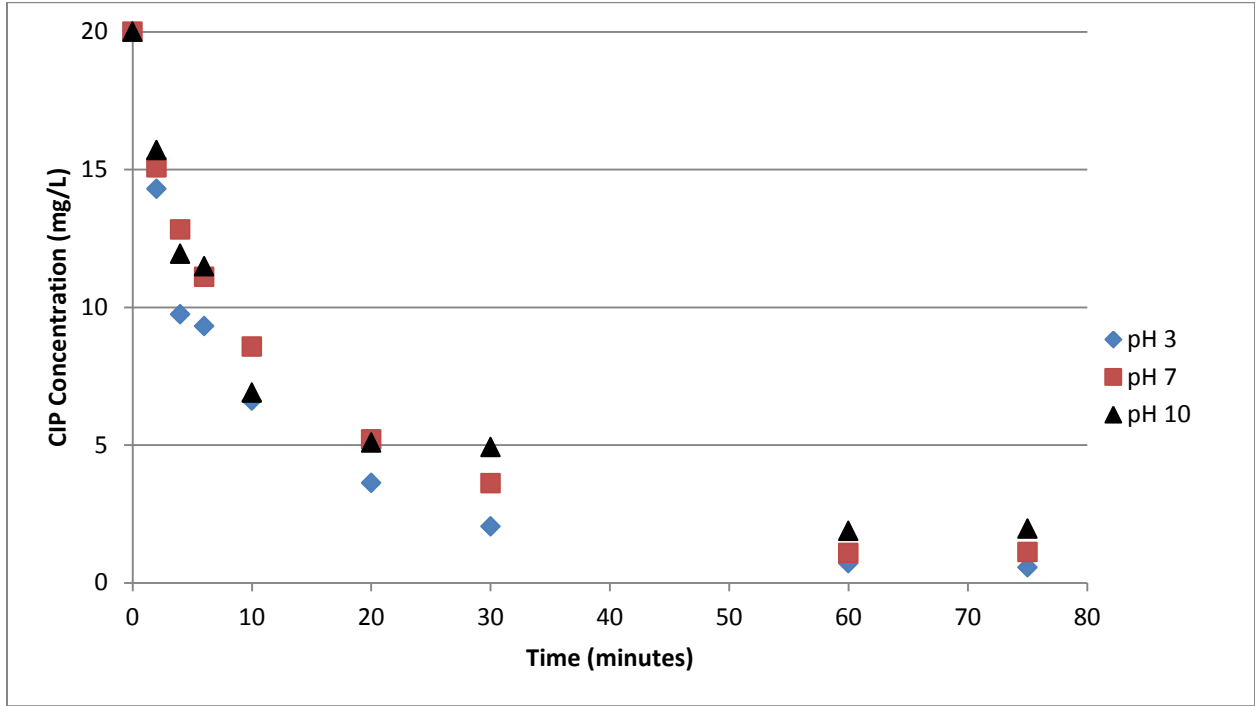


Figure 9: UV photolysis degradation at 254 nm

These data were used to determine rate constants at each pH. They were determined by the concentration of one reactant in solution with a characteristic rate constant as shown in Equation 19. This rate equation is written for batch experiments, which were conducted in this study.

$$\text{Rate of degradation} = -\frac{d[A]}{dt} = k[A] \quad (19)$$

where

$$\begin{aligned} [A] &= \text{Concentration of CIP (mg/L)} \\ t &= \text{time (min)} \\ k &= \text{rate constant (1/min)} \end{aligned}$$

The integrated form is shown in Equation 20.

$$\ln[A] = -kt + \ln[A]_0 \quad (20)$$

Therefore, the rates were determined to be first order by graphing the natural log of the final concentration of CIP vs. time, which gives a straight line with a slope of  $-k$ . Figure 10 contains the first order plots for each pH. Rate law constants for pH 3, 7, and 10 were found to be 0.0461/min ( $R^2=0.946$ ), 0.0389/min ( $R^2=0.953$ ), and 0.0297/min ( $R^2=0.893$ ), respectively. Although they are relatively close, the rate of reaction shows a decreasing trend with increasing pH. After 60 minutes of exposure to UV light with an initial CIP concentration of 20mg/L, the rate of reaction decreases to almost zero. This is because the amount of CIP remaining in solution is too small and therefore the first order rate is decreasing exponentially. In addition, it is possible that the oxygen available in the water is the limiting reactant and has been consumed, resulting in a slower or non-existent reaction.

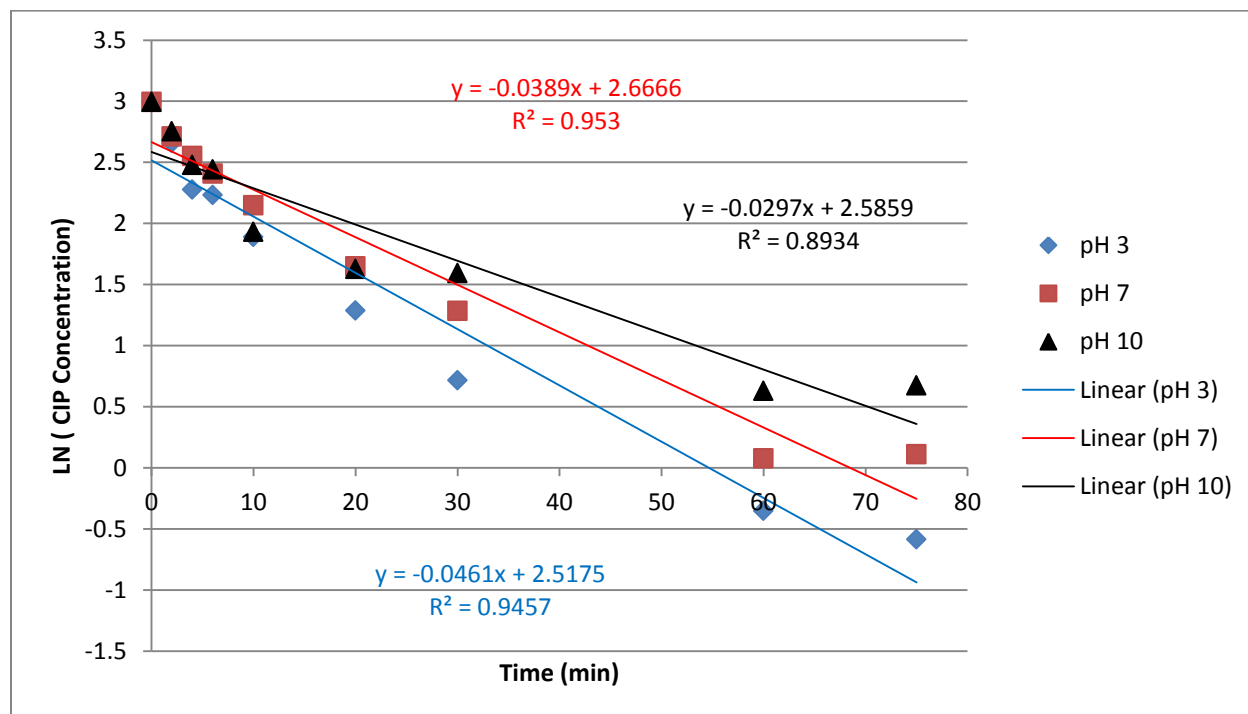


Figure 10: 1st order UV Photolysis Kinetics

#### 4.2.3 UV/H<sub>2</sub>O<sub>2</sub> Degradation

Similar experiments were conducted with UV/H<sub>2</sub>O<sub>2</sub> in order to promote the production of hydroxyl radicals. This is expected to increase the degradation rate and/or the final percent decrease of CIP in solution. The effects of hydrogen peroxide to CIP ratio as well as pH were analyzed during 45 minute trials and were compared to those with no hydrogen peroxide present.

Rate laws were found using kinetics data at all three pHs and were compared to UV photolysis experiments.

The ratio of hydrogen peroxide to CIP in solution during UV degradation is known to effect the percent removal. If there is too much hydrogen peroxide present, the competition between hydroxyl radicals and other reactants increases and CIP will not be degraded as effectively (De Witte et al., 2009). If there is not enough hydrogen peroxide, there will be an insufficient amount of hydroxyl radicals produced and therefore less available to react with CIP. In Table 2, each pH trial is shown with various ratios for comparison, including trials conducted without hydrogen peroxide. The time required to obtain approximate maximum degradation is listed. Trials were run for an additional 15 minutes to ensure that there was a negligible difference in CIP concentration with increasing time.

**Table 2: UV degradation with varying ratios of H<sub>2</sub>O<sub>2</sub>/CIP**

| <b>Molar Ratio of H<sub>2</sub>O<sub>2</sub>/Cipro</b> | <b>Required Time (min)</b> | <b>Percent Decrease at pH 3 (%)</b> | <b>Percent Decrease at pH 7 (%)</b> | <b>Percent Decrease at pH 10 (%)</b> |
|--|----------------------------|-------------------------------------|-------------------------------------|--------------------------------------|
| 100  | 30                         | 96.29                               | 93.62                               | 92.77                                |
| 50   | 30                         | 96.12                               | 96.48                               | 96.62                                |
| 10   | 30                         | 96.61                               | 89.58                               | 86.63                                |
| 5  | 30                         | 98.74                               | 84.35                               | 86.61                                |
| 1  | 30                         | 96.36                               | 86.52                               | 86.48                                |
| 0  | 60                         | 97.22                               | 94.41                               | 90.19                                |

As seen in Table 2, results for final percent removal with hydrogen peroxide and UV photolysis were relatively similar with all ratios. However, at pH 7 and pH 10, there is a slight increase in degradation at a 50 to 1 ratio. At all pHs, this ratio resulted in a high degradation percentage between 96 and 97%. Therefore, this was established as the ratio to pursue in all kinetics studies. Again, it is apparent that solutions at pH 3 are most favorable for UV degradation with and without hydrogen peroxide.

Using a 50:1 molar ratio of hydrogen peroxide to CIP and an initial CIP concentration of 20 mg/L, kinetics trials were conducted from time 0 to 45 minutes. This provided data for calculating UV/ H<sub>2</sub>O<sub>2</sub> rate laws as well as comparisons between degradation at each pH. Figure



11 contains results for these experiments, and again shows that 30 minutes was sufficient exposure time.

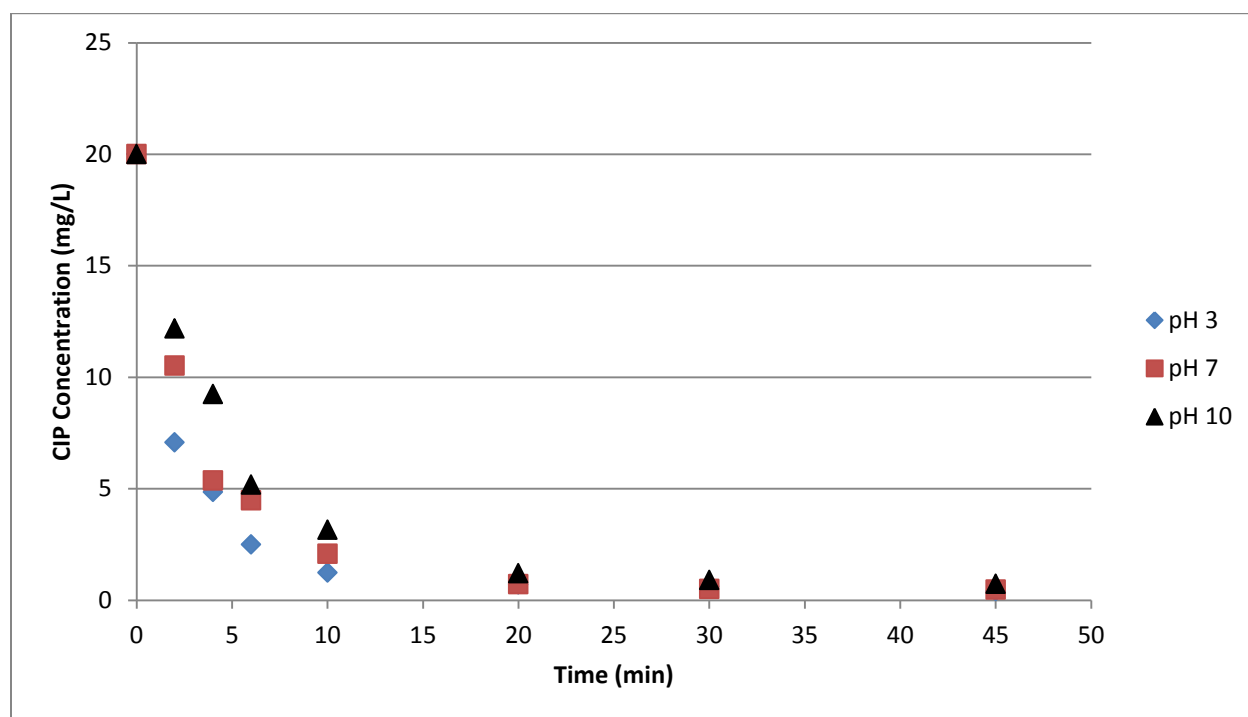


Figure 11: UV/H<sub>2</sub>O<sub>2</sub> degradation at 254 nm

The plot was used to determine rate constants at each pH. The relationship was analyzed as pseudo first order. Thus, the concentration of hydroxyl radicals was lumped into the rate constant to create a pseudo rate constant,  $k$ . According to Figure 12, the pseudo-rate constants were found to be 0.0738/min ( $R^2=0.7449$ ), 0.0804/min ( $R^2=0.8067$ ) and 0.0724/min ( $R^2=0.8393$ ) for pHs 3, 7, and 10, respectively. From the rate laws, it could be determined that pH has a very minimal effect on degradation rate. However, the data show in Figure 11 that there is a slight decrease in degradation rate with increasing pH.

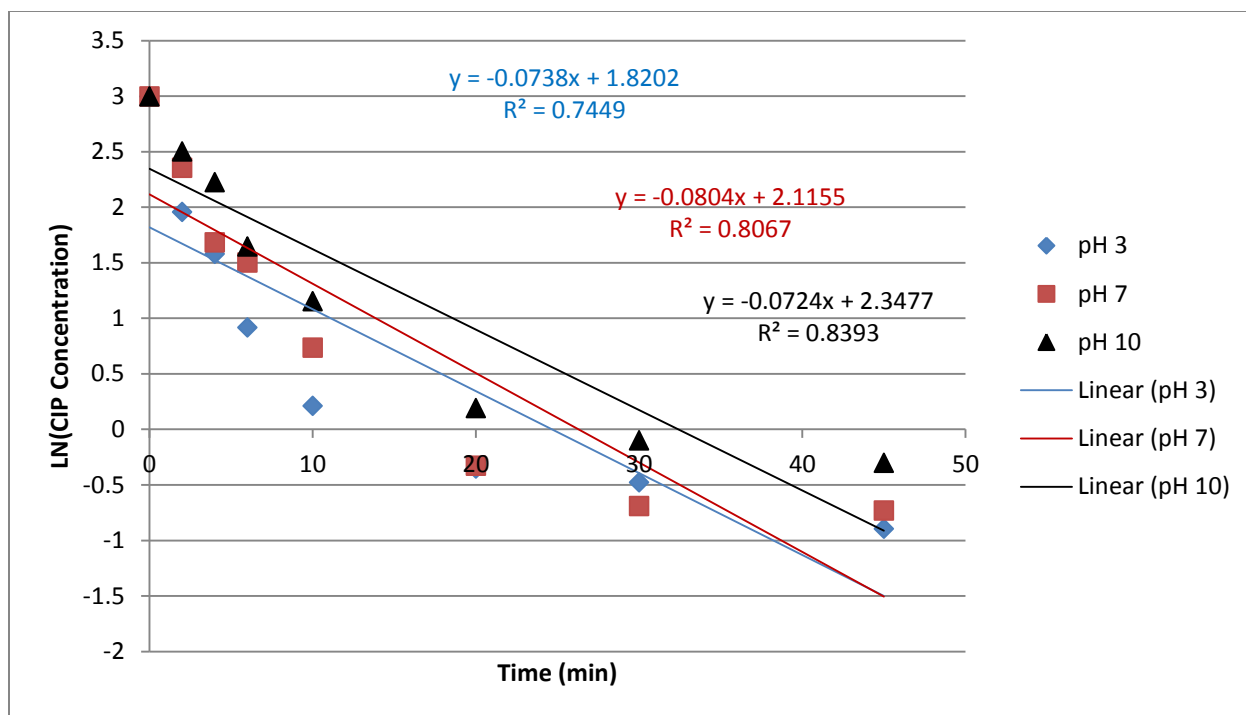


Figure 12: UV/H<sub>2</sub>O<sub>2</sub> degradation at 254 nm

#### 4.2.4 UV and UV/H<sub>2</sub>O<sub>2</sub> Degradation Comparison

Considering that UV photolysis is capable of obtaining approximately the same percentage of degradation without the addition of hydrogen peroxide, it is essential to compare the rates of these reactions to determine the benefits of adding a catalyst. Figure 13 shows a comparison of degradation rate at pH 3 with and without hydrogen peroxide. This pH was chosen due to the fact that it was the most effective throughout UV treatment.

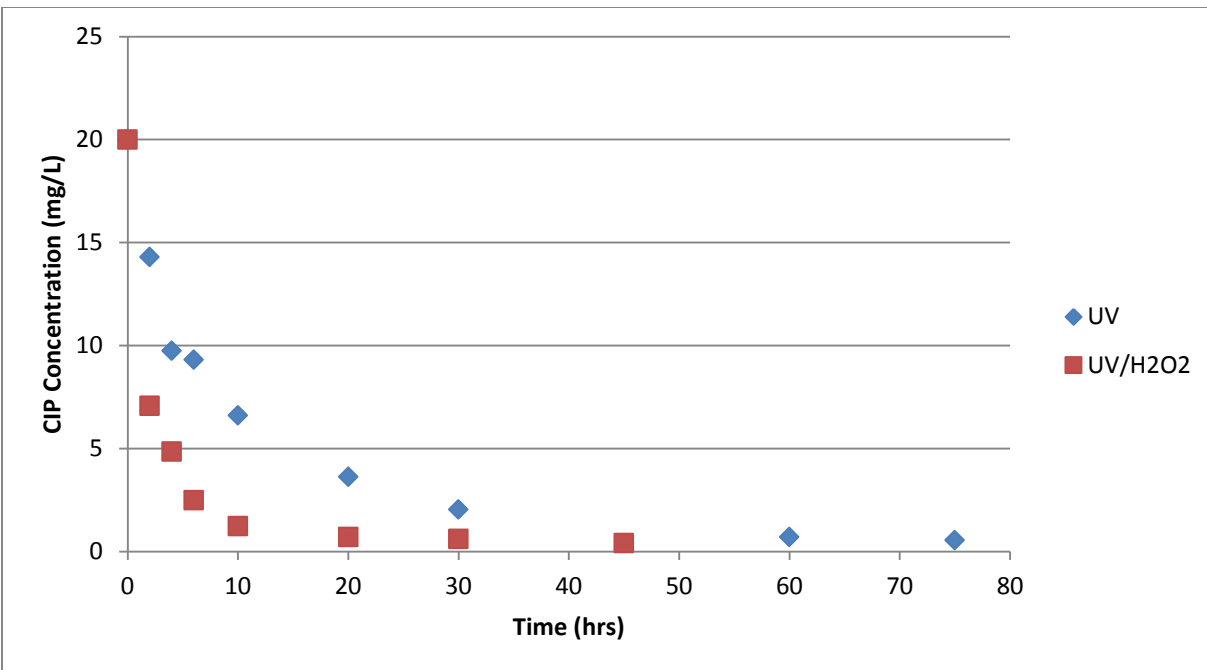


Figure 13: UV and UV/H<sub>2</sub>O<sub>2</sub> Degradation at 254 nm and pH 3

Figure 13 demonstrates that the addition of hydrogen peroxide in a H<sub>2</sub>O<sub>2</sub>:CIP molar ratio of 50:1 at pH 3 increased the rate of reaction significantly. This trend is similar for all solution pHs, as shown in Appendix C. The rate constants cannot be compared due to a difference of units; however, it is clear through visible representation in Figure 13 that the increased production of hydroxyl radicals due to the addition of hydrogen peroxide almost doubled the degradation rate of CIP.

### 4.3 Adsorption

#### 4.3.1 Adsorption Isotherms

Isotherms were generated for each activated carbon at each pH in order to establish equilibrium relationships, analyze the effect of solution pH on removal through adsorption, and compare the effectiveness of the two tested carbons.

#### Granular F600 Isotherm

Isotherm data for F600 GAC is shown in Figure 14 below.

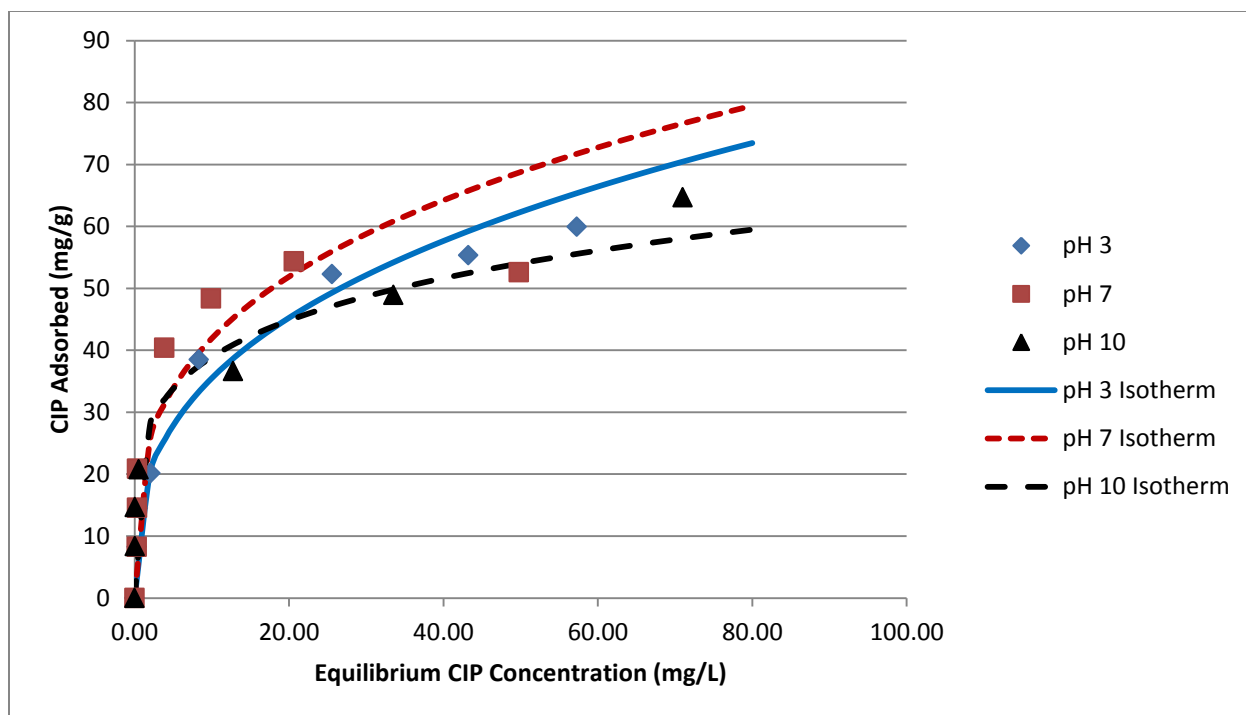


Figure 14: F600 Adsorption Isotherm

The data was modeled for both Langmuir and Freundlich isotherms and it was found to fit best to a Freundlich model. Equations 22 through 24 represent the isotherm model equations for the three data sets shown in Figure 14.

$$q = 15.876 C_e^{1/2.860} \text{ pH 3, } R^2 = 0.9647 \quad (22)$$

$$q = 20.648 C_e^{1/3.251} \text{ pH 7, } R^2=0.8257 \quad (23)$$

$$q = 24.322 C_e^{1/4.900} \text{ pH 10, } R^2=0.9483 \quad (24)$$

Under the experimental parameters tested, the isotherm at pH 7 had the highest amount of CIP adsorbed and was therefore the most effective at equilibrium. At pH 7, the zwitterionic form of CIP is dominant and thus the majority of the molecules are non-polar. This may be the reason for the higher affinity for adsorption between F600 GAC and CIP at pH 7 considering that GAC has a non-polar surface and is more likely to form bonds with a non-polar contaminant from London dispersion forces.

## Granular F200 Isotherms

Isotherm data for F200 GAC is shown in Figure 15 below.

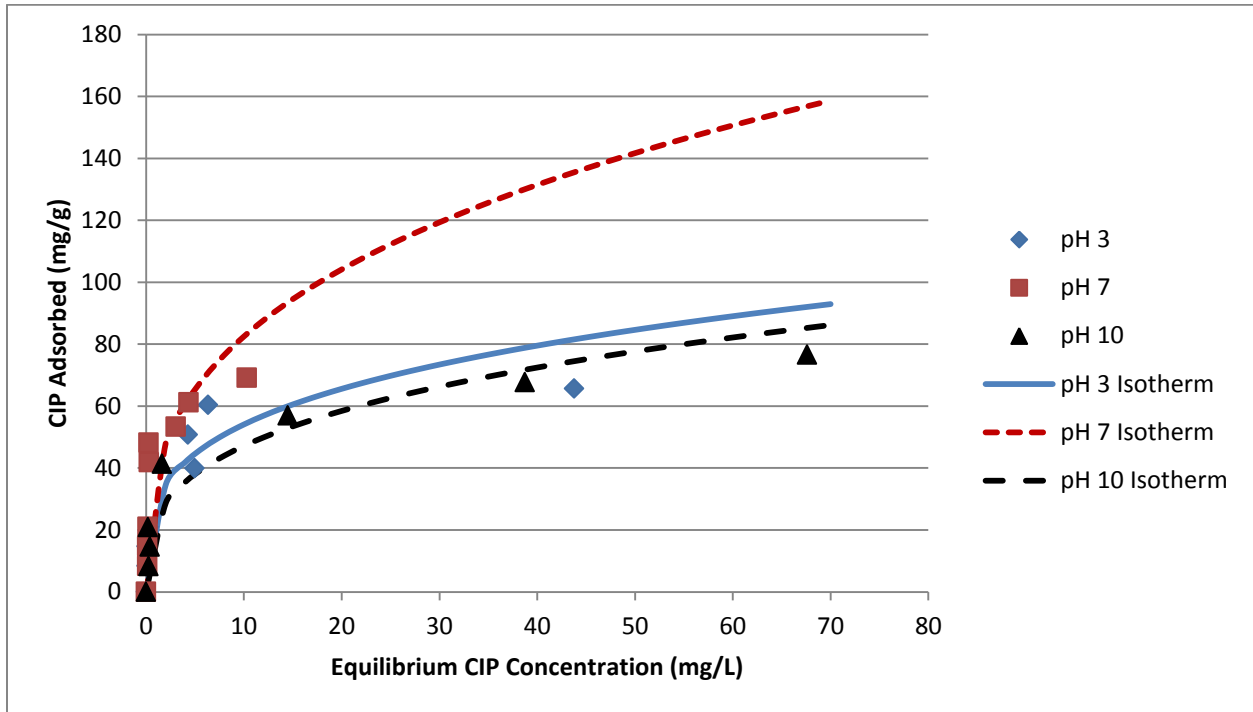


Figure 15: F200 Adsorption Isotherm

Similarly to F600 isotherms, Equations 25 through 27 shown below represent Freundlich isotherm models plotted in Figure 15.

$$q = 28.50 C_e^{1/3.595} \quad \text{pH 3, } R^2=0.7449 \quad (25)$$

$$q = 38.046 C_e^{1/2.975} \quad \text{pH 7, } R^2=0.8067 \quad (26)$$

$$q = 23.09 C_e^{1/3.226} \quad \text{pH 10, } R^2=0.8393 \quad (27)$$

The isotherms follow the same pH trends as those for F600 GAC. However, F200 GAC has overall higher  $K_f$  values at all pHs and thus a higher capacity for CIP adsorption compared to F600 GAC. The correlations were not strong, especially for isotherm models at pH 7.

Experiments at higher ratios of CIP:GAC should be conducted in order to establish a better correlation.

### 4.3.2 Adsorption Kinetics

Adsorption kinetics studies were conducted in order to ensure that 48 hours was necessary to reach equilibrium and to make comparisons with both GACs at the three pHs. In addition, data was modeled as potentially first and second order, as seen in Appendix C. However, no conclusions were drawn about specific models for this relationship due to the complex mechanism involved in adsorption. Additional studies should be conducted in order to obtain an appropriate model.

#### Granular F600 Kinetics

Figure 16 shows the kinetics data obtained for F600 GAC.

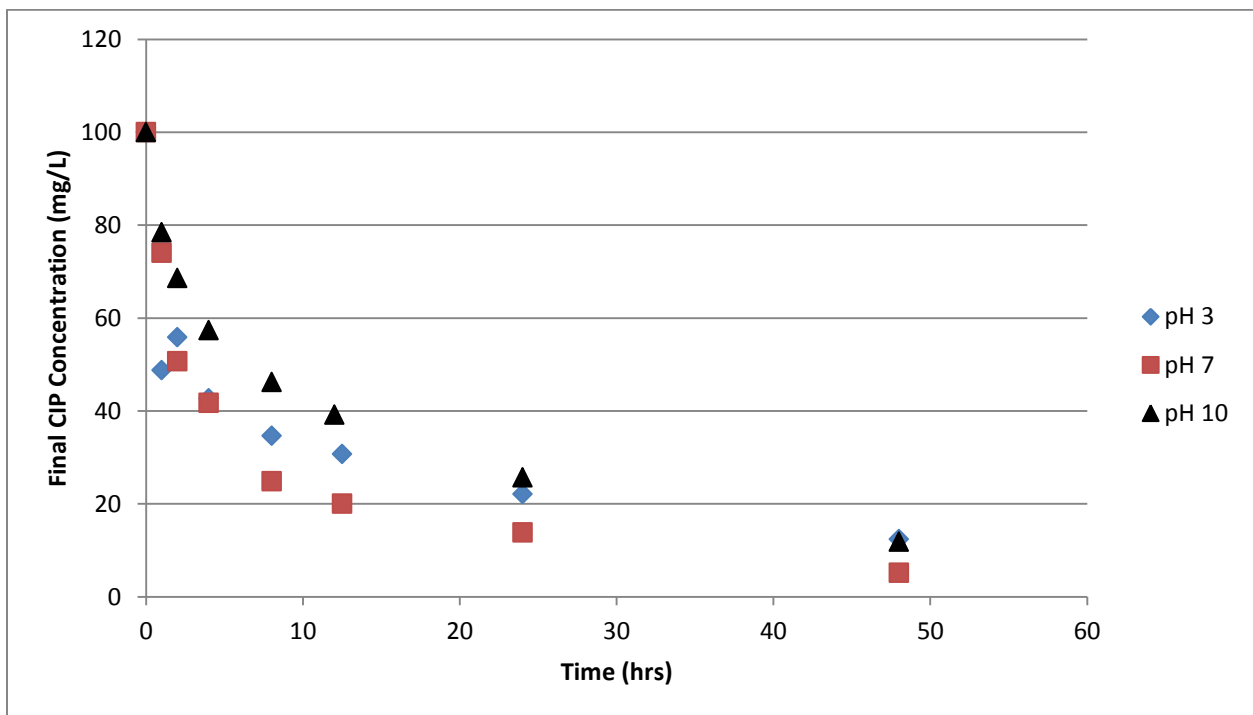


Figure 16: F600 Adsorption Kinetics

According to Figure 16, rates of removal were similar at pH 3 and 10, however removal at pH 7 occurred at more than double the rate. This is, again, most likely attributed to the non-polarity of the zwitterionic form of CIP present at pH 7.

## Granular F200 Kinetics

Kinetics data obtained for the removal of CIP by adsorption to F200GAC is shown below in Figure 17.

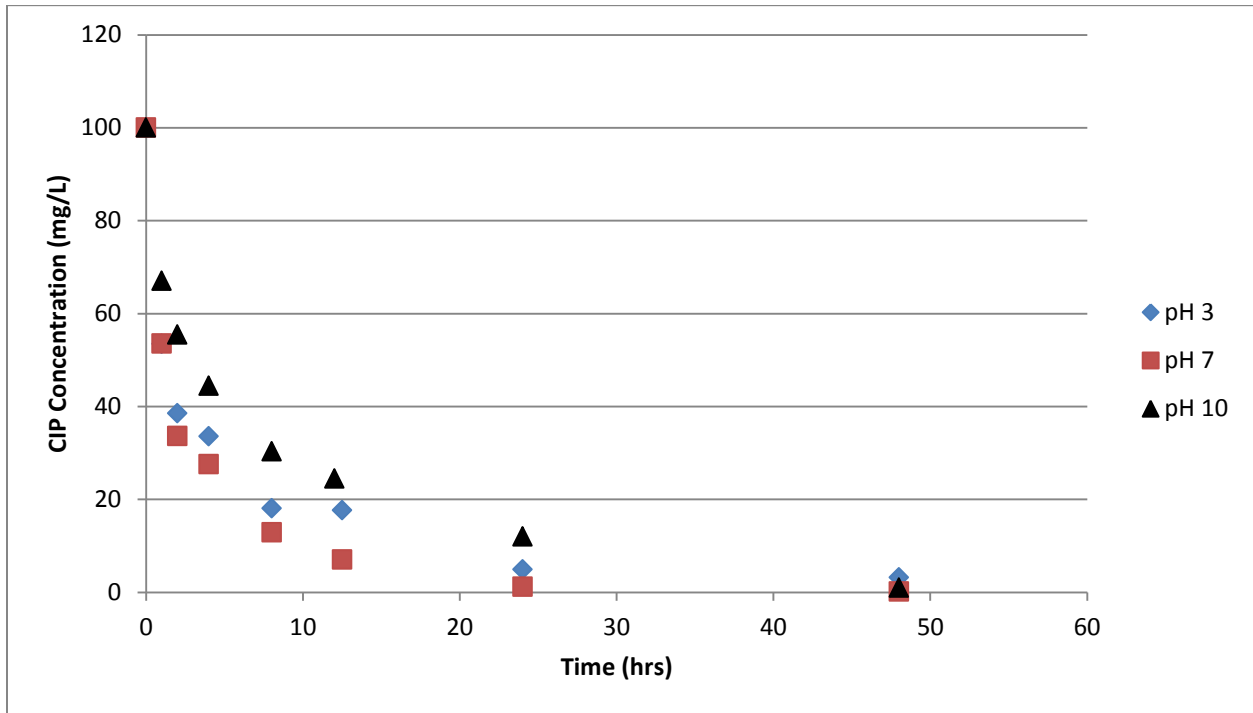


Figure 17: F200 Adsorption Kinetics

Again, adsorption treatment conducted at pH 7 was most successful in removing CIP at a higher rate compared to the other two pH ranges tested which is in agreement with all other adsorption experiments

## Comparison of Activated Carbons

Due to the success in adsorption experiments at pH 7, kinetics data at this pH from both GACs was used as a standard for comparison. Figure 18 below demonstrates this comparison.

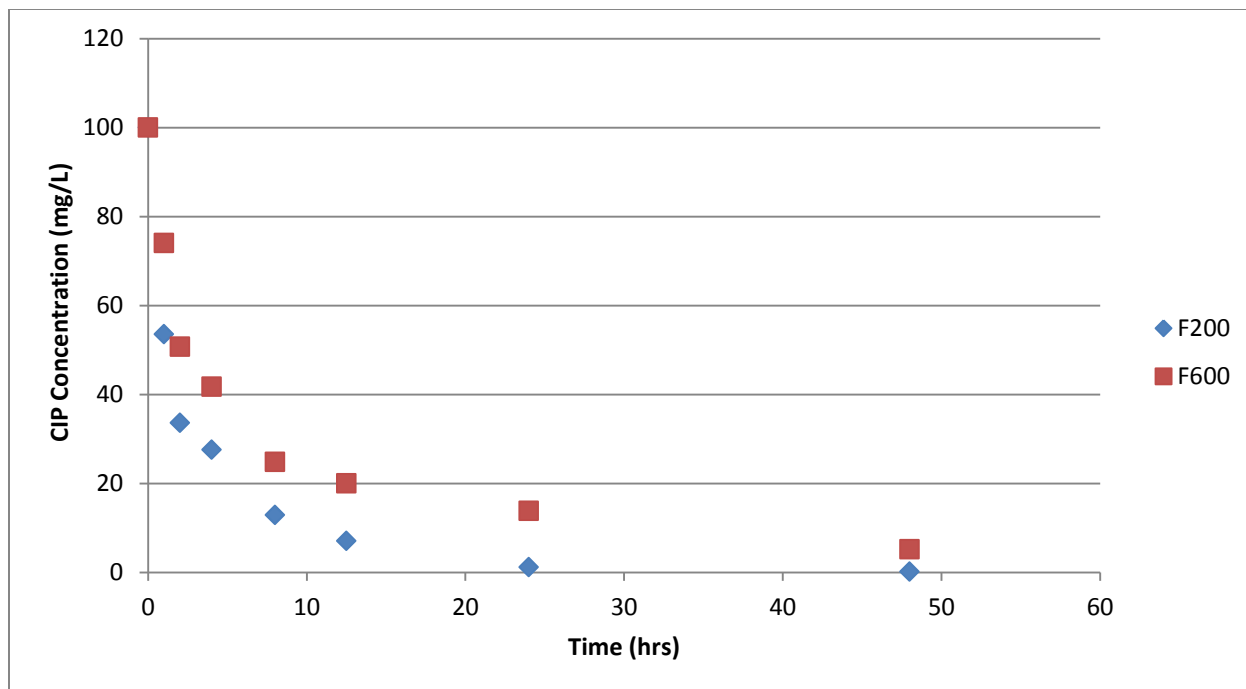


Figure 18: Comparison of Adsorption Kinetics at pH 7 for F600 and F200

Adsorption to F200 occurred at a faster rate and removed more CIP overall than F600 at the same conditions. This is in agreement with the isotherm data showing that F200 GAC is a more effective adsorbent for the removal of CIP from E-Pure water than F600 GAC. CIP is an easily adsorbed molecule due to its high molecular weight and therefore has a higher affinity for adsorbents with lower energy pores, which are pores surrounded by a lesser number of graphitic plates. Trace capacity numbers as given by Calgon Carbon Corporation represent the amount of low energy pores present in a given GAC. This relationship is directly proportional because the smaller the trace capacity number, the less energy available in the pores. The trace capacity numbers for the GACs are 11 mg/cc (min) for F200 GAC and 16 mg/cc (min) for F600 GAC. It indicates that F200 GAC has less energy pores than F600 GAC and therefore has a higher affinity for CIP. Data sheets for F200 GAC and F600 GAC can be found in Appendix D (Calgon Carbon Corporation, 2011).



## Chapter 5: Conclusions and Recommendations

All treatments analyzed in this study are potentially successful methods for removing CIP from water; however some are more effective than others. All UV treatments should be conducted at lower wavelengths (254 nm) and at pH 3, although all three pH solutions showed success in degrading CIP with UV photolysis and UV/H<sub>2</sub>O<sub>2</sub> degradation. UV photolysis follows first order kinetics while UV/H<sub>2</sub>O<sub>2</sub> obeys pseudo first order kinetics. The rate of degradation doubles with the addition of H<sub>2</sub>O<sub>2</sub>, however it degrades approximately the same percentage of CIP once equilibrium is reached.

F200 GAC was more successful at removing CIP than F600 GAC and both removed CIP faster and more effectively at pH 7. Both GACs fit to a Freundlich isotherm model with CIP; however the correlation was not always strong. Studies at higher concentrations of CIP would provide a wider range of data, which would either confirm or deny the correlation of the model.

With these conclusions in mind, further research must be conducted in order to make any definitive suggestions for treatment. It would be useful to study the effect of mixtures of antibiotics in the same solution in order to test the selectivity of these treatments. It is possible that there may be constituents in water or wastewater that attenuate UV light or scavenge hydroxyl radicals during UV treatment. It is also possible that these constituents might compete for adsorption sites during removal. It may be necessary to test treatment methods on water from an environmental source containing such mixtures.

A thorough analysis of any energy and environmental considerations involved with these treatment methods would provide an important supplement to this study. Essential parameters to consider would be the replacement and disposal of GAC, energy requirements for UV lamps, storage and cost of H<sub>2</sub>O<sub>2</sub>, and possible degradation by-products generated from UV treatment. In all treatment methods, it may not be necessary to adjust pH because the effort and cost required may not be worth the change in effectiveness of treatment. All experiments should also be conducted on a pilot and commercial scale and at environmentally relevant concentrations.

## Bibliography

- Agency, E. P. (1999). Alternative Disinfectants and Oxidants. In E. P. Agency, *EPA Guidance Manual* (pp. 1-21 (Ch. 7)).
- An, T., Yang, H., Guiying, L., Song, W., Copper, W. J., & Nie, X. (2010). Kinetics and mechanism of advanced oxidation processes (AOPs) in degradation of ciprofloxacin in water. *Applied Catalysis B: Environmental*, 288-294.
- Avisar, D., Lester, Y., & Mamane, H. (2010). pH induced polychromatic UV treatment for the removal of a mixture of SMX, OTC and CIP from water. *Journal of Hazardous Materials*, 1068-1074.
- AWWA. (1990). *Water Quality and Treatment: A Handbook of Community Water Supplies*. McGraw-Hill.
- Balcioglu, I. A., & Ötöker, M. (2003). Treatment of pharmaceutical wastewater containing antibiotics by O<sub>3</sub> and O<sub>3</sub>/H<sub>2</sub>O<sub>2</sub> processes. *Chemosphere*, 85-95.
- Batt, A. L. (2007). Comparison of the occurrence of antibiotics in four full-scale wastewater treatment plants with varying designs and operations. *Chemosphere*, 428-435.
- Bhandari, A., Close, L. I., Kim, W., Hunter, R. P., Koch, D. E., & Surampalli, R. Y. (2008). Occurrence of Ciprofloxacin, Sulfamethoxazole, and Azithromycin in Municipal Wastewater Treatment Plants. *Practice Periodical of Hazardous, Toxic, and Radioactive Waste Management*, 275-281.
- Burkholder, J., Libra, B., Weyer, P., Heathcote, S., Kolpin, D., Thome, P. S., et al. (2007). Impacts of Waste from Concentrated Animal Feeding Operations on Water Quality. *Environmental Health Perspectives*, 308-312.
- Calgon Carbon Corporation. (2011). *Calgon Carbon Corporation*. Retrieved March 7, 2011, from Activated Carbon Products and Media: <http://www.calgoncarbon.com/index.html>
- Caliman, F. A., & Gavrilescu, M. (2009). Pharmaceuticals, Personal Care Products and Endocrine Disrupting Agents in the Environment - A Review. *CLEAN – Soil, Air, Water*, 277-303.
- Carmosini, N., & Lee, L. S. (2009). Ciprofloxacin sorption by dissolved organic carbon from reference and bio-waste materials. *Chemosphere*, 812-820.
- CBWInfo.com. (2005). *Ciprofloxacin*. Retrieved March 27, 2011, from Ciprofloxacin: <http://www.cbwinfo.com/Pharmaceuticals/Cipro.html>

- Christensen, A. M., Markussen, B., Baun, A., & Halling-Sørensen, B. (2009). Probabilistic environmental risk characterization of pharmaceuticals in sewage treatment plant discharges. *Chemosphere*, 351-358.
- DailyMed. (2008, 12). *Ciprofloxacin solution/drops*. Retrieved March 27, 2011, from DailyMed:Current Medication Information: <http://dailymed.nlm.nih.gov/dailymed/drugInfo.cfm?id=8944>
- de Bel, E., Dewulf, J., De Witte, B., Langenhove, H. V., & Janssen, C. (2009). Influence of pH on the sonolysis of ciprofloxacin: Biodegradability, ecotoxicity and antibiotic activity of its degradation products. *Chemosphere*, 291-295.
- de Witte, B., Dewulf, J., Demeestere, K., & van Langenhove, H. (2009). Ozonation and advanced oxidation by the peroxone process of ciprofloxacin in water. *Journal of Hazardous Materials*, 701-708.
- De Witte, B., van Langenhove, H., Demeestere, K., Saerens, K., de Wispelaere, P., & Dewulf, J. (2010). Ciprofloxacin ozonation in hospital wastewater treatment plant effluent: Effect of pH and H<sub>2</sub>O<sub>2</sub>. *Chemosphere*, 1142-1147.
- Dodd, M. C., Buffle, M.-O., & van Gunten, U. (2009). Oxidation of Antibacterial Molecules by Aqueous Ozone: Moiety-Specific Reaction Kinetics and Application to Ozone-Based Wastewater Treatment. *Environmental Science Technology*, 1969-1977.
- Dodd, M. C., Kohler, H.-P. E., & von Gunten, U. (2009). Oxidation of Antibacterial Compounds by Ozone and Hydroxyl Radical: Elimination of Biological Activity during Aqueous Ozonation Processes. *Environmental Science Technology*, 2498-2504.
- Douglas, R. M. (1984). *Principles of Adsorption and Adsorption Process*. Wiley-Interscience.
- Elkanzi, E., & Kheng, G. B. (2000). H<sub>2</sub>O<sub>2</sub>/UV degradation kinetics of isoprene in aqueous solution. *Journal of Hazardous Materials*, 55-62.
- Fick, J., Söderström, H., Linderberg, R. H., Phan, C., Tysklind, M., & Joakim Larsson, D. (2009). Contamination of Surface, Ground, and Drinking Water from Pharmaceutical Production. *Environmental Toxicology and Chemistry*, 2522-2527.
- Gad-Allah, T. A., Ali, M. E., & Badaway, M. I. (2010). Photocatalytic oxidation of ciprofloxacin under simulated sunlight. *Journal of Hazardous Material*.
- Giger, W., Alder, A. C., Golet, E. M., Kohler, H.-P. E., McArdell, C. S., Molnar, E., et al. (2003). Occurrence and Fate of Antibiotics as Trace Contaminants in Wastewaters, Sewage Sludges, and Surface Waters. *Chimia* 57, 485-491.

- Glaze, W. H. (1986). Reaction Products of Ozone: A Review. *Environmental Health Perspectives*, 151-157.
- Golet, E. M., Alder, A. C., & Giger, W. (2002). Environmental Exposure and Risk Assessment of Fluoroquinolone Antibacterial Agents in Wastewater and River Water of the Glatt Valley Watershed, Switzerland. *Environmental Science and Technology*, 3645-3651.
- Golet, E. M., Xifra, I., Siegrist, H., Alder, A. C., & Giger, W. (2003). Environmental Exposure Assessment of Fluoroquinolone Antibacterial Agents from Sewage to Soil. *Environmental Science and Technology*, 3243-3249.
- Gros, M., Petrović, M., Ginebreda, A., & Barceló, D. (2010). Removal of pharmaceuticals during wastewater treatment and environmental risk assessment using hazard indexes. *Environmental International*, 15-26.
- Gu, C; Karthikeyan, KG. (2005). *Environmental Science Technology*, 9166-9173.
- Halling - Sørensen, B., Lützhøft, H.-C. H., H.R., A., & Ingerslev, F. (2000). Environmental risk assessment of antibiotics: comparison of mecillinam, trimethoprim and ciprofloxacin. *Journal of Antimicrobial Chemotherapy* (2000), 53-58.
- Ho, Y., & McKay, G. (1999). Pseudo-second order model for sorption processes. *Process Biochemistry*, 451-465.
- Kim, I., Yamashita, N., & Tanaka, H. (2009). Photodegradation of pharmaceuticals and personal care products during UV and UV/H<sub>2</sub>O<sub>2</sub> treatments. *Chemosphere*, 518-525.
- Kolpin, D. W., Furlong, E. T., Meyer, M. T., Thurman, E. M., Zaugg, S. D., Barber, L. B., et al. (2002). Pharmaceuticals, Hormones, and Other Organic Wastewater Contaminants in U.S. Streams, 1999-2000: A National Reconnaissance. *Environmental Science Technology*, 1202-1211.
- Legrini, O., Oliveros, E., & Braun, A. (1993). Photochemical Processes for Water Treatment. *Chemical Reviews*, 671-698.
- Letterman, R. (1999). *Water Quality and Treatment: A Handbook of Community Water Supplies*. McGraw - Hill.
- Li, B., Zhang, T., Xu, Z., & Ping Fang, H. H. (2009). Rapid analysis of 21 antibiotics of multiple classes in municipal wastewater using ultra performance liquid chromatography-tandem mass spectrometry. *Analytica Chimica Acta*, 64-72.
- Manaia, C. M., Novo, A., Coelho, B., & Nunes, O. C. (2010). Ciprofloxacin in Domestic Wastewater Treatment Plants. *Water, Air, Soil, Pollution*, 335-343.

- Martins, A. F., Vasconcelos, T. G., Henriques, D. M., Frank, C. d., König, A., & Kümmerer, K. (2008). Concentration of Ciprofloxacin in Brazilian Hospital Effluent and Preliminary Risk Assessment: A Case Study. *CLEAN – Soil, Air, Water*, 264-269.
- Maul, J. D., Schuler, L. J., Belden, J. B., Whiles, M. R., & Lydy, M. J. (2006). Effects of the Antibiotic Ciprofloxacin on Stream Microbial Communities and Detritivorous Macroinvertebrates. *Environmental Toxicology and Chemistry*, 1598-1606.
- Melo, M., Varanda, F., Dohrn, R., & Marrucho, I. (n.d.). Solubility of Ciprofloxacin and Moxifloxacin in Different Solvents: The Effect of the HCl Group. *ENPROMER*, 1-5.
- Morasch, B., Bonvin, F., Reiser, H., Grandjean, D., de Alencastro, L. F., Perazzolo, C., et al. (2010). Occurrence and Fate of Micropollutants in the Vidy Bay of Lake Geneva, Switzerland. Part II: Micropollutants Removal Between Wastewater and Raw Drinking Water. *Environmental Toxicology and Chemistry*, 29.
- Nagulapally, S. R., Ahmad, A., Henry, A., Marchin, G. L., Zurek, L., & Bhandari, A. (2008). Occurrence of Ciprofloxacin-Trimethoprim-Sulfamethoxazole-, and Vancomycin-Resistant Bacteria in Municipal Wastewater Treatment Plant. *Water Environment Research*, 82-90.
- Nakata, H., Kannan, K., Jones, P. D., & Giesy, J. P. (2005). Determination of fluoroquinolone antibiotics in wastewater effluents by liquid chromatography-mass spectrometry and fluorescence detection. *Chemosphere*, 759-766.
- Nikolaou, A., Meric, S., & Fatta, D. (2007). *Occurrence patterns of pharmaceuticals in water and wastewater environments*. Mytilene, Greece: Springer-Verlag.
- Paul, T., Dodd, M. C., & Strathmann, T. J. (2010). Photolytic and photocatalytic decomposition of aqueous ciprofloxacin: Transformation products and residual antibacterial activity. *Water Research*, 3121-3132.
- Pereira, V. J., Linden, K. G., & Weinberg, H. S. (2007). Evaluation of UV irradiation for photolytic and oxidative degradation of pharmaceutical compounds in water. *Water Research*, 4413-4423.
- Pereira, V. J., Weinberg, H. S., Linden, K. G., & Singer, P. C. (2007). UV Degradation Kinetics and Modeling of Pharmaceutical Compounds in Laboratory Grade and Surface Water via Direct and Indirect Photolysis at 254 nm. *Environmental Science Technology*, 1682-1688.
- Plósz, B. G., Leknes, H., & Thomas, K. V. (2010). Impacts of Competitive Inhibition, Parent Compound Formation and Partitioning Behavior on the Removal of Antibiotics in Municipal Wastewater Treatment. *Environmental Science Technology*, 734-742.

- Plósz, B. G., Leknes, H., Liltved, H., & Thomas, K. V. (2010). Diurnal variations in the occurrence and the fate of hormones and antibiotics in activated sludge wastewater treatment in Oslo, Norway. *Science of the Total Environment*, 1915-1924.
- Punyapalakul, P., & Sitthisorn, T. (2010). Removal of Ciprofloxacin and Carbamazepine by Adsorption on Functionalized Mesoporous Silicates. *World Academy of Science, Engineering and Technology*, 546-550.
- Richards, S. M., Wilson, C. J., Johnson, D. J., Castle, D. M., Lam, M., Mabury, S. A., et al. (2004). Effects of Pharmaceutical Mixtures in Aquatic Microcosms. *Environmental Toxicology and Chemistry*, 1035-1042.
- Robinson, A. A., Belden, J. B., & Lydy, M. J. (2005). Toxicity of Fluoroquinolone Antibiotics to Aquatic Organisms. *Environmental Toxicology and Chemistry*, 423-430.
- Rogue-Malherbe, R. M. (2007). *Adsorption and Diffusion in Nanoporous Materials*. CRC.
- Schwartz, T., Volkmann, H., Kirchen, S., Kohnen, W., Schön-Hölz, K., Jansen, B., et al. (2006). *Real-Time PCR detection of Pseudomonas aeruginosa in clinical and municipal wastewater and genotyping of the ciprofloxacin-resistant isolates*. Karlsruhe, Germany: Blackwell Publishing Ltd.
- Shi, L., Zhou, X., Yalei, Z., & Gu, G. (n.d.). Occurrence and Removal of Fluoroquinolone Antibiotics in a Sewage Treatment Plant in Shanghai, China. Shanghai, China.
- Sim, W.-J., Lee, J.-W., & Oh, J.-E. (2010). Occurrence and date of pharmaceuticals in wastewater treatment plants and rivers in Korea. *Environmental Pollution*, 1938-1947.
- Snyder, S. A., Westerhoff, P., Yoon, Y., & Sedlak, D. L. (2003). Pharmaceuticals, Personal Care Products, and Endocrine Disruptors in Water: Implications for the Water Industry. *Environmental Engineering Science*, 449 - 469.
- Suarez, M., Entenza, J., Doerries, C., Meyer, E., Bourquin, L., Sutherland, J., et al. (2003). Expression of a Plant-Derived Peptide Harboring Water-Cleaning and Antimicrobial Activities. *Biotechnology and Bioengineering*.
- Sun, S.-P., Guo, H.-Q., Ke, Q., Sun, J.-H., Shi, S.-H., & Zhang, M.-L. Z. (2009). Degradation of Antibiotic Ciprofloxacin Hydrochloride by Photo-Fenton Oxidation Process. *Environmental Engineering Science*, 753-759.
- U.S. Department of the Interior Bureau of Reclamation. (2009). *Secondary/Emerging Constituents*. U.S Department of the Interior.
- van Doorslaer, X., Demeestere, K., Heynderickx, P. M., van Langenhove, H., & Dewulf, J. (2011). UV-A and UV-C induced photolytic and photocatalytic degradation of aqueous

- ciprofloxacin and moxifloxacin: Reaction kinetics and role of adsorption. *Applied Catalysis B: Environmental*, 540-547.
- Vasconcelos, T. G., Kümmerer, K., Henriques, D. M., & Martins, A. F. (2009). Ciprofloxacin in hospital effluent: Degradation by ozone and photoprocesses. *Journal of Hazardous Materials*, 1154-1158.
- Vieno, N. M., Härkki, H., & Tuhkanen, K. L. (2007). Occurrence of Pharmaceuticals in River Water and Their Elimination in a Pilot-Scale Drinking Water Treatment Plant. *Environmental Science Technology*, 5077-5084.
- Watkinson, A., Murby, E., & Costanzo, S. (2007). Removal of antibiotics in conventional and advanced wastewater treatment: Implications for environmental discharge and wastewater recycling. *Water Research*, 4164-4176.
- Wu, Q., Zhaohui, L., Hong, H., Yin, K., & Tie, L. (2010). Adsorption and intercalation of ciprofloxacin on montmorillonite. *Applied Clay Science*, 204-211.
- Yang, R. T. (2003). *Adsorbents: Fundamentals and Applications*. Wiley-Interscience.
- Yuan, F., Hu, C., Hu, X., Wei, D., Chen, Y., & Qu, J. (2011). Photodegradation and toxicity changes of antibiotics in UV and UV/H<sub>2</sub>O<sub>2</sub> process. *Journal of Hazardous Materials*, 1256-1263.
- Zhang, Huichun; Huang, Ching-Hua. (2007). *Adsorption and oxidation of fluoroquinolone antibacterial agents and structurally related amines with goethite*, 1502-1512.
- Zieliwicz, E. (2008). Sonolysis and Sonoacidification of Ultrasonic Disintegration of Excess Sludge. *Acta Physica Polonica A*, 259-264.
- Zorita, S., Mårtensson, L., & Mathiasson, L. (2009). Occurrence and removal of pharmaceuticals in a municipal sewage treatment system in the south of Sweden. *Science of the Total Environment*, 2760-2770.
- Zuccato, E., Castiglioni, S., Bagnati, R., Melis, M., & Fanelli, R. (2010). Source, occurrence and fate of antibiotics in the Italian aquatic environment. *Journal of Hazardous Materials*, 1042-1048.
- Zuccato, E., Castiglioni, S., Bagnati, R., Melis, M., & Fanelli, R. (2010). Source, occurrence and fate of antibiotics in the Italian aquatic environment. *Journal of Hazardous Materials*, 1042-1048.

## **Appendix A –Glossary of Terms**

AOP – Advanced Oxidation Processes

API –Active Pharmaceutical Ingredients

CEC – Compounds of Emerging Concern

CIP – Ciprofloxacin Hydrochloride

EDC – Endocrine Disrupting Chemical

ETTP – Enhanced Tertiary Treatment Processes

FQ - Fluoroquinolone

GAC – Granular Activated Carbon

HRT – Hydraulic Retention Time

LOAEL – Lowest Observed Adverse Effect Level

LOQ – Limits of Quantification

MIC – Minimum Inhibitory Concentration

NOAEL – No Observed Adverse Effect Level

NOM – Natural Organic Matter

PhAC- Pharmaceutically Active Compound

PCP – Personal Care Products

PPCP – Pharmaceutical and Personal Care Products

SPE – Solid Phase Extraction

TOC – Total Organic Carbon

USEPA – United States Environmental Protection Agency

UV – Ultraviolet

WWTP – Waste Water Treatment Plant



## Appendix B - Raw Data

### Calibration Curves

Table 3: Calibration Curves

| Measured Concentration of CIP (mg/L) | pH   | Absorbance | pH   | Absorbance | pH    | Absorbance |
|--------------------------------------|------|------------|------|------------|-------|------------|
| 20.000                               | 3.01 | 2.501      | 7.04 | 1.679      | 9.99  | 1.259      |
| 10.000                               | 3.02 | 1.271      | 6.99 | 0.755      | 9.98  | 0.590      |
| 5.000                                | 2.99 | 0.604      | 7.01 | 0.432      | 10.03 | 0.278      |
| 2.500                                | 3.02 | 0.385      | 6.99 | 0.211      | 10.02 | 0.131      |
| 1.250                                | 2.99 | 0.192      | 6.97 | 0.087      | 10.02 | 0.072      |
| 0.625                                | 3.01 | 0.092      | 7.05 | 0.049      | 10.03 | 0.038      |
| 0.313                                | 3.01 | 0.045      | 7.04 | 0.025      | 10.02 | 0.019      |
| 0.156                                | 3.01 | 0.034      | 7.04 | 0.015      | 10.03 | 0.009      |
| 0.078                                | 3.00 | 0.020      | 7.00 | 0.007      | 10.03 | 0.004      |
| 0.039                                | 2.99 | 0.011      | 6.96 | 0.005      | 9.98  | 0.003      |

### UV Photolysis at 365nm

Table 4: UV Photolysis at 365 nm

| Total Time (min) | pH <sub>i</sub> | pH <sub>f</sub> | Abs <sub>f</sub> | Conc <sub>i</sub> (mg/L) | Conc <sub>f</sub> (mg/L) | ΔConc (mg/L) | % Decrease |
|------------------|-----------------|-----------------|------------------|--------------------------|--------------------------|--------------|------------|
| 75               | 3.01            | 3.02            | 1.688            | 20                       | 13.430                   | 6.570        | 32.848     |
| 75               | 7.02            | 7.01            | 1.220            | 20                       | 14.808                   | 5.192        | 25.959     |
| 75               | 9.98            | 10.01           | 1.145            | 20                       | 18.559                   | 1.441        | 7.204      |

### UV Photolysis Kinetics at 254 nm

Table 5: UV Photolysis Kinetics at pH 3

| Total Time (min) | pH <sub>i</sub> | pH <sub>f</sub> | Conc <sub>i</sub> (mg/L) | Abs <sub>f</sub> | Conc <sub>f</sub> (mg/L) | ΔConc (mg/L) | % Decrease |
|------------------|-----------------|-----------------|--------------------------|------------------|--------------------------|--------------|------------|
| 0                | 3.07            | 3.07            | 20                       | -                | 20.000                   | 0            | 0          |
| 2                | 3.07            | 3.04            | 20                       | 1.797            | 14.294                   | 5.706        | 28.532     |
| 4                | 3.07            | 3.05            | 20                       | 1.225            | 9.748                    | 10.252       | 51.261     |
| 6                | 3.07            | 3.07            | 20                       | 1.171            | 9.314                    | 10.686       | 53.429     |
| 10               | 3.07            | 3.03            | 20                       | 0.831            | 6.610                    | 13.390       | 66.949     |
| 20               | 3.07            | 3.03            | 20                       | 0.456            | 3.625                    | 16.375       | 81.877     |
| 30               | 3.07            | 3               | 20                       | 0.257            | 2.044                    | 17.956       | 89.781     |
| 60               | 3.03            | 3.02            | 20                       | 0.088            | 0.703                    | 19.297       | 96.484     |
| 75               | 3.03            | 3.02            | 20                       | 0.070            | 0.557                    | 19.443       | 97.216     |

Table 6: UV Photolysis Kinetics at pH 7

| Total Time (min) | pH <sub>i</sub> | pH <sub>f</sub> | Conc <sub>i</sub> (mg/L) | Abs <sub>f</sub> | Conc <sub>f</sub> (mg/L) | ΔConc (mg/L) | % Decrease |
|------------------|-----------------|-----------------|--------------------------|------------------|--------------------------|--------------|------------|
| 0                | 7.01            | 7.01            | 20.0000                  | -                | 20                       | 0            | 0          |
| 2                | 7.01            | 6.95            | 20                       | 1.242            | 15.070                   | 4.930        | 24.648     |
| 4                | 7.01            | 6.98            | 20                       | 1.056            | 12.820                   | 7.180        | 35.898     |
| 6                | 7.01            | 7.02            | 20                       | 0.915            | 11.107                   | 8.893        | 44.466     |
| 10               | 7.01            | 6.97            | 20                       | 0.707            | 8.576                    | 11.424       | 57.118     |
| 20               | 7.01            | 7               | 20                       | 0.429            | 5.203                    | 14.797       | 73.987     |
| 30               | 7.01            | 7.01            | 20                       | 0.298            | 3.614                    | 16.386       | 81.930     |
| 60               | 7.01            | 7.02            | 20                       | 0.089            | 1.079                    | 18.921       | 94.606     |
| 75               | 7.01            | 7.02            | 20                       | 0.092            | 1.118                    | 18.882       | 94.411     |

Table 7: UV Photolysis Kinetics at pH 10

| Total Time (min) | pH <sub>i</sub> | pH <sub>f</sub> | Conc <sub>i</sub> (mg/L) | Abs <sub>f</sub> | Conc <sub>f</sub> (mg/L) | ΔConc (mg/L) | % Decrease |
|------------------|-----------------|-----------------|--------------------------|------------------|--------------------------|--------------|------------|
| 0                | 10.01           | 10.01           | 20                       | -                | 20                       | 0            | 0          |
| 2                | 10.01           | 9.98            | 20                       | 0.969            | 15.703                   | 4.297        | 21.483     |
| 4                | 10.01           | 9.95            | 20                       | 0.737            | 11.940                   | 8.060        | 40.300     |
| 6                | 10.01           | 9.96            | 20                       | 0.709            | 11.485                   | 8.515        | 42.577     |
| 10               | 10.01           | 9.95            | 20                       | 0.426            | 6.896                    | 13.104       | 65.519     |
| 20               | 10.01           | 9.99            | 20                       | 0.314            | 5.086                    | 14.914       | 74.571     |
| 30               | 10.01           | 10.04           | 20                       | 0.304            | 4.921                    | 15.079       | 75.397     |
| 60               | 10.01           | 10.03           | 20                       | 0.116            | 1.877                    | 18.123       | 90.616     |
| 75               | 10.02           | 10.03           | 20                       | 0.121            | 1.963                    | 18.037       | 90.186     |

## UV/H<sub>2</sub>O<sub>2</sub> Degradation

Table 8: UV /H<sub>2</sub>O<sub>2</sub> Degradation at pH 3

| Molar Ratio of H <sub>2</sub> O <sub>2</sub> /CIP | Total Time (min) | pH <sub>i</sub> | pH <sub>f</sub> | Conc <sub>i</sub> (mg/L) | Abs <sub>f</sub> | Conc <sub>f</sub> (mg/L) | ΔConc (mg/L) | % Decrease |
|---|------------------|-----------------|-----------------|--------------------------|------------------|--------------------------|--------------|------------|
| 100   | 30               | 3.01            | 2.99            | 20                       | 0.074            | 0.588                    | 19.412       | 97.060     |
| 50  | 30               | 3.04            | 3.03            | 20                       | 0.096            | 0.763                    | 19.237       | 96.185     |
| 10  | 30               | 3.04            | 3.04            | 20                       | 0.084            | 0.667                    | 19.333       | 96.667     |
| 5   | 30               | 3.02            | 3.03            | 20                       | 0.026            | 0.207                    | 19.793       | 98.966     |
| 1   | 30               | 3.01            | 3.03            | 20                       | 0.075            | 0.599                    | 19.401       | 97.005     |

Table 9: UV /H2O2 Degradation at pH 7

| Molar Ratio of H2O2/CIP | Total Time (min) | pH <sub>i</sub> | pH <sub>f</sub> | Conc <sub>i</sub> (mg/L) | Abs <sub>f</sub> | Conc <sub>f</sub> (mg/L) | ΔConc (mg/L) | % Decrease |
|-------------------------|------------------|-----------------|-----------------|--------------------------|------------------|--------------------------|--------------|------------|
| 100                     | 30               | 7.01            | 6.99            | 20                       | 0.079            | 0.960                    | 19.040       | 95.200     |
| 50                      | 30               | 7.01            | 7.02            | 20                       | 0.041            | 0.501                    | 19.499       | 97.494     |
| 10                      | 30               | 6.99            | 6.99            | 20                       | 0.125            | 1.522                    | 18.478       | 92.391     |
| 5                       | 30               | 7.01            | 7.03            | 20                       | 0.188            | 2.286                    | 17.714       | 88.568     |
| 1                       | 30               | 7.01            | 7.03            | 20                       | 0.158            | 1.919                    | 18.081       | 90.407     |

Table 10: UV /H2O2 Degradation at pH 10

| Molar Ratio of H2O2/CIP | Total Time (min) | pH <sub>i</sub> | pH <sub>f</sub> | Conc <sub>i</sub> (mg/L) | Abs <sub>f</sub> | Conc <sub>f</sub> (mg/L) | ΔConc (mg/L) | % Decrease |
|-------------------------|------------------|-----------------|-----------------|--------------------------|------------------|--------------------------|--------------|------------|
| 100                     | 30               | 10.02           | 10.01           | 20                       | 0.119            | 1.445                    | 18.555       | 92.773     |
| 50                      | 30               | 9.99            | 10.03           | 20                       | 0.056            | 0.676                    | 19.324       | 96.620     |
| 10                      | 30               | 10.02           | 10.01           | 20                       | 0.220            | 2.675                    | 17.325       | 86.626     |
| 5                       | 30               | 9.96            | 10.01           | 20                       | 0.221            | 2.677                    | 17.323       | 86.614     |
| 1                       | 30               | 9.98            | 9.96            | 20                       | 0.223            | 2.704                    | 17.296       | 86.481     |

### UV/H<sub>2</sub>O<sub>2</sub> Degradation – Kinetics

Table 11: UV /H2O2 Degradation Kinetics at pH 3

| Total Time (min) | pH <sub>i</sub> | pH <sub>f</sub> | Conc <sub>i</sub> (mg/L) | Abs <sub>f</sub> | Conc <sub>f</sub> (mg/L) | ΔConc (mg/L) | % Decrease |
|------------------|-----------------|-----------------|--------------------------|------------------|--------------------------|--------------|------------|
| 0                | 3.03            | 3.03            | 20                       | -                | 20                       | 0            | 0          |
| 2                | 3.03            | 3.04            | 20                       | 0.889            | 7.073                    | 12.927       | 64.634     |
| 4                | 3.03            | 3.05            | 20                       | 0.609            | 4.847                    | 15.153       | 75.764     |
| 6                | 3.03            | 3.05            | 20                       | 0.314            | 2.496                    | 17.504       | 87.518     |
| 10               | 3.03            | 3.05            | 20                       | 0.155            | 1.235                    | 18.765       | 93.827     |
| 20               | 3.03            | 3.01            | 20                       | 0.088            | 0.701                    | 19.299       | 96.496     |
| 30               | 3.03            | 3.05            | 20                       | 0.078            | 0.621                    | 19.379       | 96.897     |
| 45               | 3.03            | 3.05            | 20                       | 0.051            | 0.408                    | 19.592       | 97.959     |

Table 12: UV /H2O2 Degradation Kinetics at pH 7

| <u>Total Time</u><br>(min) | <u>pH<sub>i</sub></u> | <u>pH<sub>f</sub></u> | <u>Conc<sub>i</sub></u><br>(mg/L) | <u>Abs<sub>f</sub></u> | <u>Conc<sub>f</sub></u><br>(mg/L) | <u>ΔConc</u><br>(mg/L) | <u>%</u><br><u>Decrease</u> |
|----------------------------|-----------------------|-----------------------|-----------------------------------|------------------------|-----------------------------------|------------------------|-----------------------------|
| 0                          | 7.04                  | 7.04                  | 20                                | -                      | 20                                | 0                      | 0                           |
| 2                          | 7.04                  | 7.01                  | 20                                | 0.867                  | 10.524                            | 9.476                  | 47.379                      |
| 4                          | 7.04                  | 7.01                  | 20                                | 0.443                  | 5.370                             | 14.630                 | 73.149                      |
| 6                          | 7.04                  | 6.97                  | 20                                | 0.369                  | 4.481                             | 15.519                 | 77.597                      |
| 10                         | 7.04                  | 6.96                  | 20                                | 0.172                  | 2.086                             | 17.914                 | 89.569                      |
| 20                         | 7.04                  | 6.98                  | 20                                | 0.059                  | 0.720                             | 19.280                 | 96.402                      |
| 30                         | 7.01                  | 7.02                  | 20                                | 0.041                  | 0.501                             | 19.499                 | 97.494                      |
| 45                         | 7.02                  | 7.01                  | 20                                | 0.040                  | 0.481                             | 19.519                 | 97.597                      |

Table 13: UV /H2O2 Degradation Kinetics at pH 10

| <u>Total Time</u><br>(min) | <u>pH<sub>i</sub></u> | <u>pH<sub>f</sub></u> | <u>Conc<sub>i</sub></u><br>(mg/L) | <u>Abs<sub>f</sub></u> | <u>Conc<sub>f</sub></u><br>(mg/L) | <u>ΔConc</u><br>(mg/L) | <u>%</u><br><u>Decrease</u> |
|----------------------------|-----------------------|-----------------------|-----------------------------------|------------------------|-----------------------------------|------------------------|-----------------------------|
| 0                          | 9.97                  | 9.97                  | 20                                | -                      | 20                                | 0                      | 0                           |
| 2                          | 9.97                  | 9.96                  | 20                                | 0.752                  | 12.191                            | 7.809                  | 39.044                      |
| 4                          | 9.97                  | 9.96                  | 20                                | 0.570                  | 9.237                             | 10.763                 | 53.817                      |
| 6                          | 9.97                  | 9.97                  | 20                                | 0.320                  | 5.186                             | 14.814                 | 74.068                      |
| 10                         | 9.97                  | 10.01                 | 20                                | 0.195                  | 3.160                             | 16.840                 | 84.198                      |
| 20                         | 9.97                  | 9.97                  | 20                                | 0.075                  | 1.211                             | 18.789                 | 93.947                      |
| 30                         | 9.97                  | 10.04                 | 20                                | 0.056                  | 0.904                             | 19.096                 | 95.478                      |
| 45                         | 9.97                  | 10.05                 | 20                                | 0.046                  | 0.739                             | 19.261                 | 96.305                      |

### Adsorption - F600 Isotherm

Table 14: F600 Isotherm at pH 3

| <u>Mass</u><br><u>of AC</u><br>(g) | <u>Total</u><br><u>Time</u><br>(hrs) | <u>pH<sub>i</sub></u> | <u>pH<sub>f</sub></u> | <u>Conc<sub>i</sub></u><br>(mg/L) | <u>Abs<sub>f</sub></u> | <u>Conc<sub>f</sub></u><br>(mg/L) | <u>ΔConc</u><br>(mg/L) | <u>%</u><br><u>Decrease</u> | <u>CIP</u><br><u>Adsorbed</u><br>(mg/g) |
|------------------------------------|--------------------------------------|-----------------------|-----------------------|-----------------------------------|------------------------|-----------------------------------|------------------------|-----------------------------|---|
| 0                                  | 0                                    | -                     | -                     | 0                                 | -                      | 0.00                              | 0                      | 0                           | 0                                       |
| 0.10                               | 48                                   | 3.01                  | 3.02                  | 20                                | 0.037                  | 0.298                             | 19.702                 | 98.512                      | 8.275                                   |
| 0.10                               | 48                                   | 3.03                  | 3.01                  | 35                                | 0.056                  | 0.446                             | 34.554                 | 98.727                      | 14.513                                  |
| 0.10                               | 48                                   | 3.03                  | 2.98                  | 50                                | 0.258                  | 2.053                             | 47.947                 | 95.895                      | 20.138                                  |
| 0.10                               | 48                                   | 3.02                  | 3.02                  | 100                               | 1.047                  | 8.330                             | 91.670                 | 91.670                      | 38.501                                  |
| 0.10                               | 48                                   | 3.03                  | 3.03                  | 150                               | 3.214                  | 25.570                            | 124.430                | 82.954                      | 52.261                                  |
| 0.10                               | 48                                   | 3.03                  | 3.02                  | 175                               | 5.432                  | 43.215                            | 131.785                | 75.306                      | 55.350                                  |
| 0.10                               | 48                                   | 3.03                  | 3.01                  | 200                               | 7.20                   | 57.279                            | 142.721                | 71.360                      | 59.943                                  |

Table 15: F600 Isotherm at pH 7

| <u>Mass of AC</u><br>(g) | <u>Total Time</u><br>(hrs) | <u>pH<sub>i</sub></u> | <u>pH<sub>f</sub></u> | <u>Conc<sub>i</sub></u><br>(mg/L) | <u>Abs<sub>f</sub></u> | <u>Conc<sub>f</sub></u><br>(mg/L) | <u>ΔConc</u><br>(mg/L) | <u>% Decrease</u> | <u>CIP Adsorbed</u><br>(mg/g) |
|--------------------------|----------------------------|-----------------------|-----------------------|-----------------------------------|------------------------|-----------------------------------|------------------------|-------------------|-------------------------------|
| 0                        | 0                          | -                     | -                     | 0                                 | -                      | 0                                 | 0                      | 0                 | 0                             |
| 0.10                     | 48                         | 7.02                  | 6.96                  | 20                                | 0.024                  | 0.285                             | 19.715                 | 98.574            | 8.280                         |
| 0.10                     | 48                         | 6.97                  | 6.97                  | 35                                | 0.027                  | 0.328                             | 34.672                 | 99.064            | 14.562                        |
| 0.10                     | 48                         | 7.04                  | 7.00                  | 50                                | 0.026                  | 0.318                             | 49.682                 | 99.364            | 20.866                        |
| 0.10                     | 48                         | 6.98                  | 6.96                  | 100                               | 0.318                  | 3.859                             | 96.141                 | 96.141            | 40.379                        |
| 0.10                     | 48                         | 7.02                  | 7.02                  | 125                               | 0.814                  | 9.879                             | 115.121                | 92.097            | 48.351                        |
| 0.10                     | 48                         | 6.96                  | 6.98                  | 150                               | 1.701                  | 20.646                            | 129.354                | 86.236            | 54.329                        |
| 0.10                     | 48                         | 7.01                  | 6.98                  | 175                               | 4.101                  | 49.769                            | 125.231                | 71.560            | 52.597                        |

Table 16: F600 Isotherm at pH 10

| <u>Mass of AC</u><br>(g) | <u>Total Time</u><br>(hrs) | <u>pH<sub>i</sub></u> | <u>pH<sub>f</sub></u> | <u>Conc<sub>i</sub></u><br>(mg/L) | <u>Abs<sub>f</sub></u> | <u>Conc<sub>f</sub></u><br>(mg/L) | <u>ΔConc</u><br>(mg/L) | <u>% Decrease</u> | <u>CIP Adsorbed</u><br>(mg/g) |
|--------------------------|----------------------------|-----------------------|-----------------------|-----------------------------------|------------------------|-----------------------------------|------------------------|-------------------|-------------------------------|
| 0                        | 0                          | -                     | -                     | 0                                 | -                      | 0.00                              | 0                      | 0                 | 0                             |
| 0.10                     | 48                         | 9.97                  | 10.01                 | 20                                | 0.001                  | <0.06                             | 19.983                 | 99.917            | 8.393                         |
| 0.10                     | 48                         | 9.98                  | 9.98                  | 35                                | 0.001                  | <0.06                             | 34.978                 | 99.938            | 14.691                        |
| 0.10                     | 48                         | 9.96                  | 10.02                 | 50                                | 0.033                  | 0.535                             | 49.465                 | 98.930            | 20.775                        |
| 0.10                     | 48                         | 9.98                  | 9.96                  | 100                               | 0.788                  | 12.776                            | 87.224                 | 87.224            | 36.634                        |
| 0.10                     | 48                         | 9.93                  | 9.99                  | 150                               | 2.069                  | 33.533                            | 116.467                | 77.645            | 48.916                        |
| 0.10                     | 48                         | 10.03                 | 9.96                  | 225                               | 4.380                  | 70.989                            | 154.011                | 68.449            | 64.685                        |

### Adsorption – F200 Isotherm

Table 17: F200 Isotherm at pH 3

| <u>Mass of AC</u><br>(g) | <u>Total Time</u><br>(hrs) | <u>pH<sub>i</sub></u> | <u>pH<sub>f</sub></u> | <u>Conc<sub>i</sub></u><br>(mg/L) | <u>Abs<sub>f</sub></u> | <u>Conc<sub>f</sub></u><br>(mg/L) | <u>ΔConc</u><br>(mg/L) | <u>% Decrease</u> | <u>CIP Adsorbed</u><br>(mg/g) |
|--------------------------|----------------------------|-----------------------|-----------------------|-----------------------------------|------------------------|-----------------------------------|------------------------|-------------------|-------------------------------|
| 0                        | 0                          | -                     | -                     | 0                                 | -                      | 0                                 | 0                      | 0                 | 0                             |
| 0.1                      | 48                         | 3.01                  | 2.98                  | 20                                | 0.007                  | <0.06                             | 19.946                 | 99.730            | 8.377                         |
| 0.1                      | 48                         | 3.03                  | 2.96                  | 35                                | 0.005                  | <0.06                             | 34.960                 | 99.886            | 14.683                        |
| 0.1                      | 48                         | 3.03                  | 3.02                  | 50                                | 0.029                  | 0.232                             | 49.768                 | 99.535            | 20.902                        |
| 0.1                      | 48                         | 3.02                  | 3.04                  | 100                               | 0.622                  | 4.944                             | 95.056                 | 95.056            | 39.923                        |
| 0.1                      | 48                         | 3.03                  | 3.02                  | 125                               | 0.537                  | 4.274                             | 120.726                | 96.581            | 50.705                        |
| 0.1                      | 48                         | 3.03                  | 3.02                  | 150                               | 0.797                  | 6.337                             | 143.663                | 95.776            | 60.339                        |
| 0.1                      | 48                         | 3.03                  | 2.97                  | 200                               | 5.504                  | 43.787                            | 156.213                | 78.107            | 65.610                        |

Table 18: F200 Isotherm at pH 7

| <u>Mass of AC</u><br>(g) | <u>Total Time</u><br>(hrs) | <u>pH<sub>i</sub></u> | <u>pH<sub>f</sub></u> | <u>Conc<sub>i</sub></u><br>(mg/L) | <u>Abs<sub>f</sub></u> | <u>Conc<sub>f</sub></u><br>(mg/L) | <u>ΔConc</u><br>(mg/L) | <u>% Decrease</u> | <u>CIP Adsorbed</u><br>(mg/g) |
|--------------------------|----------------------------|-----------------------|-----------------------|-----------------------------------|------------------------|-----------------------------------|------------------------|-------------------|-------------------------------|
| 0                        | 0                          | -                     | -                     | 0                                 | -                      | 0                                 | 0                      | 0                 | 0                             |
| 0.1                      | 48                         | 7.02                  | 7.03                  | 20                                | 0.009                  | 0.106                             | 19.894                 | 99.472            | 8.356                         |
| 0.1                      | 48                         | 6.97                  | 7.02                  | 35                                | 0.011                  | 0.130                             | 34.870                 | 99.629            | 14.645                        |
| 0.1                      | 48                         | 7.04                  | 7.03                  | 50                                | 0.013                  | 0.161                             | 49.839                 | 99.677            | 20.932                        |
| 0.1                      | 48                         | 6.98                  | 7.04                  | 100                               | 0.023                  | 0.273                             | 99.727                 | 99.727            | 41.885                        |
| 0.1                      | 48                         | 6.94                  | 7                     | 115                               | 0.020                  | 0.237                             | 114.763                | 99.794            | 48.201                        |
| 0.1                      | 48                         | 6.95                  | 6.99                  | 130                               | 0.249                  | 3.025                             | 126.975                | 97.673            | 53.329                        |
| 0.1                      | 48                         | 6.96                  | 7.02                  | 150                               | 0.359                  | 4.353                             | 145.647                | 97.098            | 61.172                        |
| 0.1                      | 48                         | 7.01                  | 6.98                  | 175                               | 0.849                  | 10.297                            | 164.703                | 94.116            | 69.175                        |

Table 19: F200 Isotherm at pH 10

| <u>Mass of AC</u><br>(g) | <u>Total Time</u><br>(hrs) | <u>pH<sub>i</sub></u> | <u>pH<sub>f</sub></u> | <u>Conc<sub>i</sub></u><br>(mg/L) | <u>Abs<sub>f</sub></u> | <u>Conc<sub>f</sub></u><br>(mg/L) | <u>ΔConc</u><br>(mg/L) | <u>% Decrease</u> | <u>CIP Adsorbed</u><br>(mg/g) |
|--------------------------|----------------------------|-----------------------|-----------------------|-----------------------------------|------------------------|-----------------------------------|------------------------|-------------------|-------------------------------|
| 0                        | 0                          | -                     | -                     | 0                                 | -                      | 0                                 | 0                      | 0                 | 0                             |
| 0.1                      | 48                         | 9.97                  | 9.98                  | 20                                | 0.016                  | 0.259                             | 19.741                 | 98.703            | 8.291                         |
| 0.1                      | 48                         | 9.98                  | 10                    | 35                                | 0.023                  | 0.373                             | 34.627                 | 98.935            | 14.543                        |
| 0.1                      | 48                         | 9.96                  | 10                    | 50                                | 0.011                  | 0.185                             | 49.815                 | 99.630            | 20.922                        |
| 0.1                      | 48                         | 9.98                  | 9.97                  | 100                               | 0.101                  | 1.639                             | 98.361                 | 98.361            | 41.312                        |
| 0.1                      | 48                         | 9.93                  | 9.94                  | 150                               | 0.894                  | 14.496                            | 135.504                | 90.336            | 56.912                        |
| 0.1                      | 48                         | 9.97                  | 10                    | 200                               | 2.391                  | 38.744                            | 161.256                | 80.628            | 67.728                        |
| 0.1                      | 48                         | 9.98                  | 9.95                  | 250                               | 4.171                  | 67.593                            | 182.407                | 72.963            | 76.611                        |

### Adsorption - F600 Kinetics

Table 20: F600 Adsorption Kinetics at pH 3

| <u>Vial #</u> | <u>Conc</u> (mg/L) | <u>Time</u> (hrs) | <u>pH<sub>i</sub></u> | <u>pH<sub>f</sub></u> | <u>Abs<sub>f</sub></u> | <u>Conc<sub>f</sub></u> (mg/L) |
|---------------|--------------------|-------------------|-----------------------|-----------------------|------------------------|--------------------------------|
| 0             | 100                | 0                 | 3.03                  | 3.03                  | -                      | 100                            |
| 1             | 100                | 1                 | 3.03                  | 3.02                  | 6.127                  | 48.74303898                    |
| 2             | 100                | 2                 | 3.03                  | 3.01                  | 7.0265                 | 55.89896579                    |
| 3             | 100                | 4                 | 3.03                  | 3.03                  | 5.365                  | 42.68098648                    |
| 4             | 100                | 8                 | 3.03                  | 3.04                  | 4.3585                 | 34.67382657                    |
| 5             | 100                | 12.5              | 3.03                  | 3.02                  | 3.866                  | 30.7557677                     |
| 6             | 100                | 24                | 3.03                  | 3.03                  | 2.7815                 | 22.12808274                    |
| 7             | 100                | 48                | 3.03                  | 3.02                  | 1.5549                 | 12.3699284                     |

**Table 21: F600 Adsorption Kinetics at pH 7**

| <b>Vial #</b> | <b>Conc (mg/L)</b> | <b>Time (hrs)</b> | <b>pH<sub>i</sub></b> | <b>pH<sub>f</sub></b> | <b>Abs<sub>f</sub></b> | <b>Conc<sub>f</sub> (mg/L)</b> |
|---------------|--------------------|-------------------|-----------------------|-----------------------|------------------------|--------------------------------|
| 0             | 100                | 0                 | 6.99                  | 6.99                  | -                      | 100                            |
| 8             | 100                | 1                 | 6.99                  | 7.02                  | 6.1                    | 74.02912621                    |
| 9             | 100                | 2                 | 6.99                  | 7.03                  | 4.1805                 | 50.7342233                     |
| 10            | 100                | 4                 | 6.99                  | 6.97                  | 3.439                  | 41.73543689                    |
| 11            | 100                | 8                 | 6.99                  | 6.95                  | 2.0485                 | 24.86043689                    |
| 12            | 100                | 12.5              | 6.99                  | 7.03                  | 1.6515                 | 20.04247573                    |
| 13            | 100                | 24                | 6.99                  | 6.97                  | 1.142                  | 13.8592233                     |
| 14            | 100                | 48                | 6.99                  | 7.02                  | 0.4262                 | 5.172330097                    |

**Table 22: F600 Adsorption Kinetics at pH 10**

| <b>Vial #</b> | <b>Conc (mg/L)</b> | <b>Time (hrs)</b> | <b>pH<sub>i</sub></b> | <b>pH<sub>f</sub></b> | <b>Abs<sub>f</sub></b> | <b>Conc<sub>f</sub> (mg/L)</b> |
|---------------|--------------------|-------------------|-----------------------|-----------------------|------------------------|--------------------------------|
| 0             | 100                | 0                 | 10.04                 | 10.04                 | -                      | 100                            |
| 1             | 100                | 1                 | 10.04                 | 10.02                 | 4.84                   | 78.44408428                    |
| 2             | 100                | 2                 | 10.04                 | 10.05                 | 4.2345                 | 68.63047002                    |
| 3             | 100                | 4                 | 10.04                 | 10.02                 | 3.5395                 | 57.36628849                    |
| 4             | 100                | 8                 | 10.04                 | 10.03                 | 2.85                   | 46.19124797                    |
| 5             | 100                | 12                | 10.04                 | 9.96                  | 2.42                   | 39.22204214                    |
| 6             | 100                | 24                | 10.04                 | 9.95                  | 1.5846                 | 25.68233387                    |
| 7             | 100                | 48                | 10.04                 | 9.96                  | 0.73                   | 11.83144246                    |

### Adsorption - F200 Kinetics

**Table 23: F200 Adsorption Kinetics at pH 3**

| <b>Vial #</b> | <b>Conc (mg/L)</b> | <b>Time (hrs)</b> | <b>pH<sub>i</sub></b> | <b>pH<sub>f</sub></b> | <b>Abs<sub>f</sub></b> | <b>Conc<sub>f</sub> (mg/L)</b> |
|---------------|--------------------|-------------------|-----------------------|-----------------------|------------------------|--------------------------------|
| 0             | 100                | 0                 | 3.03                  | 3.03                  | -                      | 100                            |
| 1             | 100                | 1                 | 3.03                  | 3.02                  | 6.7185                 | 53.44868735                    |
| 2             | 100                | 2                 | 3.03                  | 3.03                  | 4.841                  | 38.51233095                    |
| 3             | 100                | 4                 | 3.03                  | 3.05                  | 4.218                  | 33.55608592                    |
| 4             | 100                | 8                 | 3.03                  | 3.03                  | 2.271                  | 18.06682578                    |
| 5             | 100                | 12.5              | 3.03                  | 3.02                  | 2.22                   | 17.66109785                    |
| 6             | 100                | 24                | 3.03                  | 2.99                  | 0.611                  | 4.860779634                    |
| 7             | 100                | 48                | 3.03                  | 3.02                  | 0.3998                 | 3.180588703                    |

**Table 24: F200 Adsorption Kinetics at pH 7**

| <b>Vial #</b> | <b>Conc (mg/L)</b> | <b>Time (hrs)</b> | <b>pH<sub>i</sub></b> | <b>pH<sub>f</sub></b> | <b>Abs<sub>f</sub></b> | <b>Conc<sub>f</sub> (mg/L)</b> |
|---------------|--------------------|-------------------|-----------------------|-----------------------|------------------------|--------------------------------|
| 0             | 100                | 0                 | 6.99                  | 6.99                  | -                      | 100                            |
| 8             | 100                | 1                 | 6.99                  | 6.97                  | 4.411                  | 53.5315534                     |
| 9             | 100                | 2                 | 6.99                  | 7.02                  | 2.7715                 | 33.63470874                    |
| 10            | 100                | 4                 | 6.99                  | 6.96                  | 2.2715                 | 27.56674757                    |
| 11            | 100                | 8                 | 6.99                  | 6.96                  | 1.0605                 | 12.87014563                    |
| 12            | 100                | 12.5              | 6.99                  | 7.04                  | 0.58                   | 7.038834951                    |
| 13            | 100                | 24                | 6.99                  | 6.99                  | 0.0945                 | 1.14684466                     |
| 14            | 100                | 48                | 6.99                  | 7.01                  | 0.0141                 | 0.171116505                    |

**Table 25: F200 Adsorption Kinetics at pH 10**

| <b>Vial #</b> | <b>Conc (mg/L)</b> | <b>Time (hrs)</b> | <b>pH<sub>i</sub></b> | <b>pH<sub>f</sub></b> | <b>Abs<sub>f</sub></b> | <b>Conc<sub>f</sub> (mg/L)</b> |
|---------------|--------------------|-------------------|-----------------------|-----------------------|------------------------|--------------------------------|
| 0             | 100                | 0                 | 10.04                 | 10.04                 | -                      | 100                            |
| 1             | 100                | 1                 | 10.04                 | 9.95                  | 4.1355                 | 67.02593193                    |
| 2             | 100                | 2                 | 10.04                 | 9.95                  | 3.421                  | 55.44570502                    |
| 3             | 100                | 4                 | 10.04                 | 10.02                 | 2.74                   | 44.40842788                    |
| 4             | 100                | 8                 | 10.04                 | 10.01                 | 1.87                   | 30.30794165                    |
| 5             | 100                | 12                | 10.04                 | 9.95                  | 1.508                  | 24.44084279                    |
| 6             | 100                | 24                | 10.04                 | 9.96                  | 0.7398                 | 11.99027553                    |
| 7             | 100                | 48                | 10.04                 | 10.02                 | 0.0575                 | 0.931928687                    |



## Appendix C: Sample Calculations

### Detection Limit

Table 26: Detection Limit Data

| CIP Conc. (mg/L) | Zero   | 1      | 0.5    | 0.25   | 0.1    | 0.08   | 0.06   | 0.05    |
|------------------|--------|--------|--------|--------|--------|--------|--------|---------|
| Absorbance       | 0      | 0.0742 | 0.408  | 0.0167 | 0.0067 | 0.0043 | 0.0004 | -0.0067 |
|                  | 0.0003 | 0.0743 | 0.0411 | 0.0167 | 0.0063 | 0.0044 | 0.0004 | -0.0063 |
|                  | 0.0003 | 0.0742 | 0.0411 | 0.0167 | 0.0062 | 0.0044 | 0.0003 | -0.0062 |
|                  | 0      | 0.0744 | 0.0409 | 0.0167 | 0.0062 | 0.0042 | 0.0005 | -0.0062 |
|                  | 0.0002 | 0.0745 | 0.0411 | 0.0167 | 0.0059 | 0.0043 | 0.0005 | -0.0059 |

Table 27: t-Test: Paired Two Sample for Means

| t-Test: Paired Two Sample for Means |            |            |
|-------------------------------------|------------|------------|
|                                     | Variable 1 | Variable 2 |
| Mean                                | 0.0002     | 0.00042    |
| Variance                            | 2E-08      | 7E-09      |
| Observations                        | 5          | 5          |
| Pearson Correlation                 | -0.507     |            |
| Hypothesized Mean Difference        | 0.0001     |            |
| df                                  | 4          |            |
| t Stat                              | -4.142     |            |
| P(T<=t) one-tail                    | 0.0072     |            |
| t Critical one-tail                 | 2.1318     |            |
| P(T<=t) two-tail                    | 0.0144     |            |
| t Critical two-tail                 | 2.7764     |            |

# Adsorption Isotherms

## F600

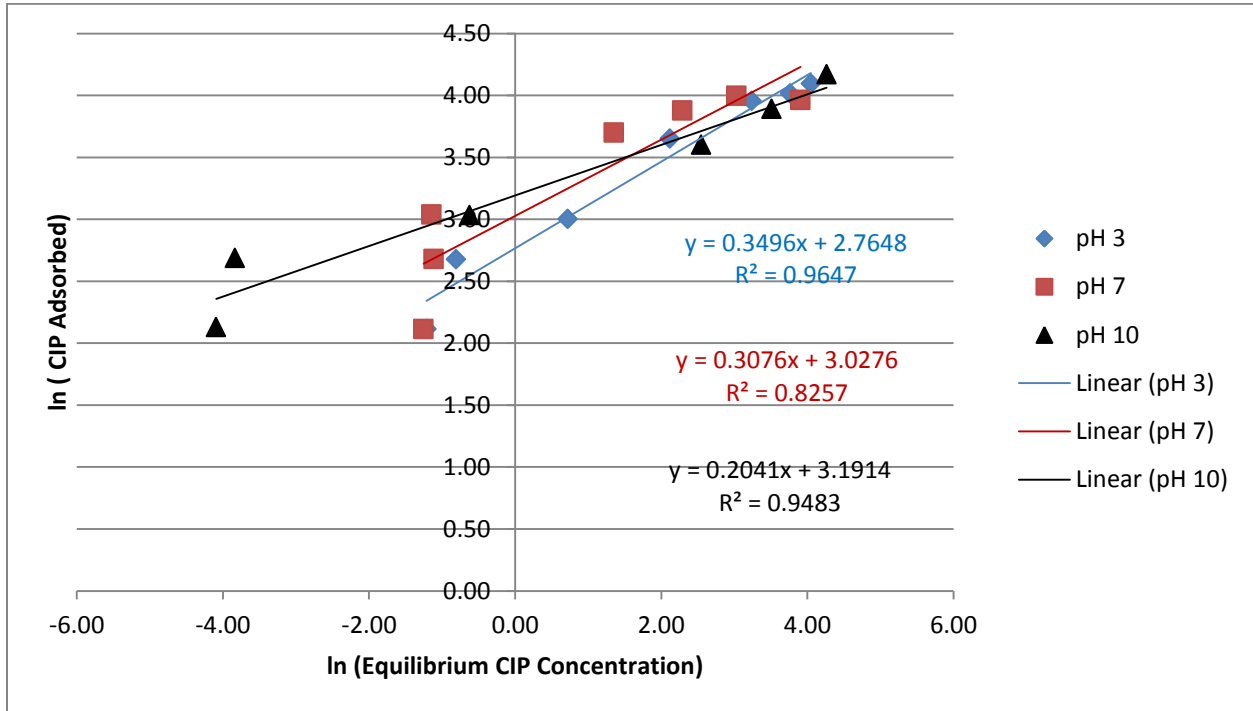


Figure 19: F600 Freundlich Isotherm

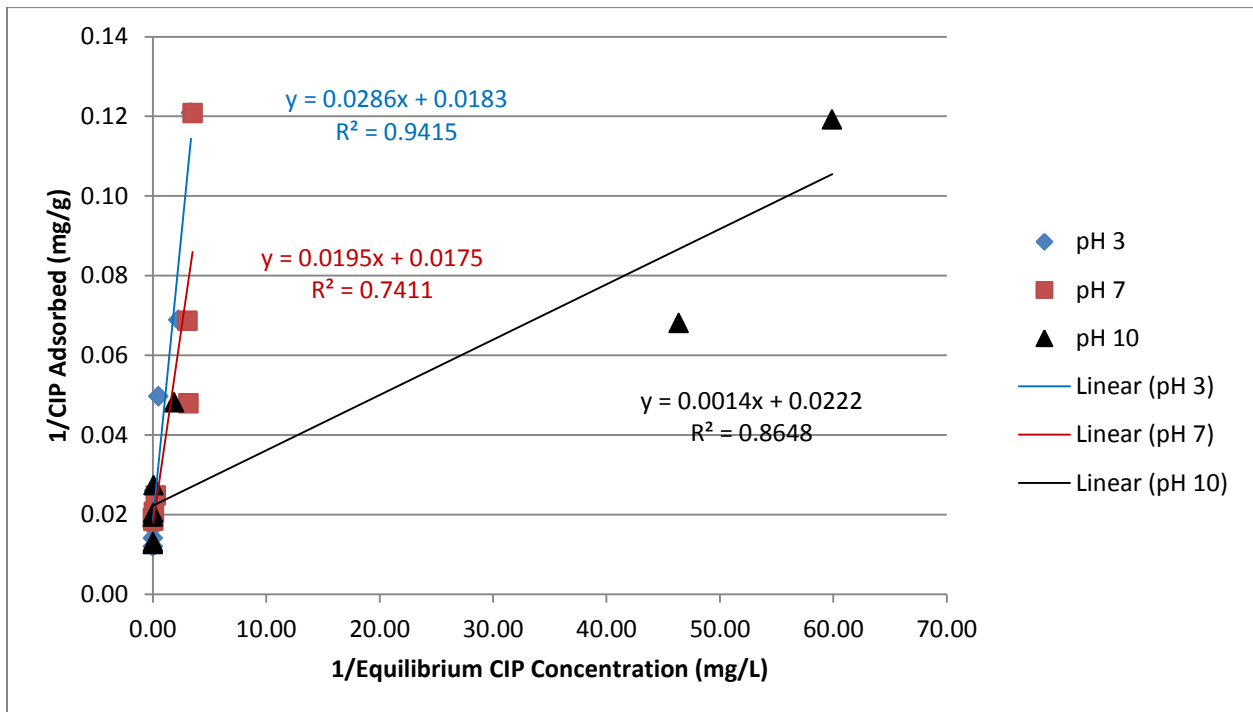
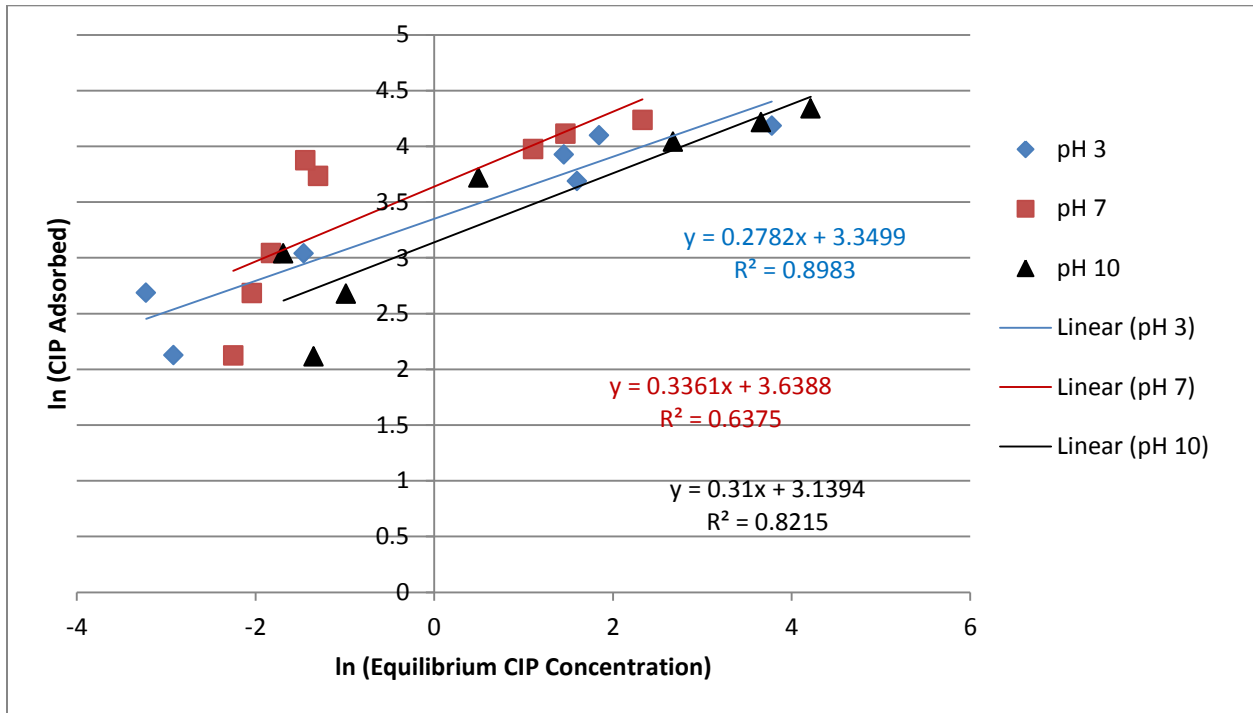
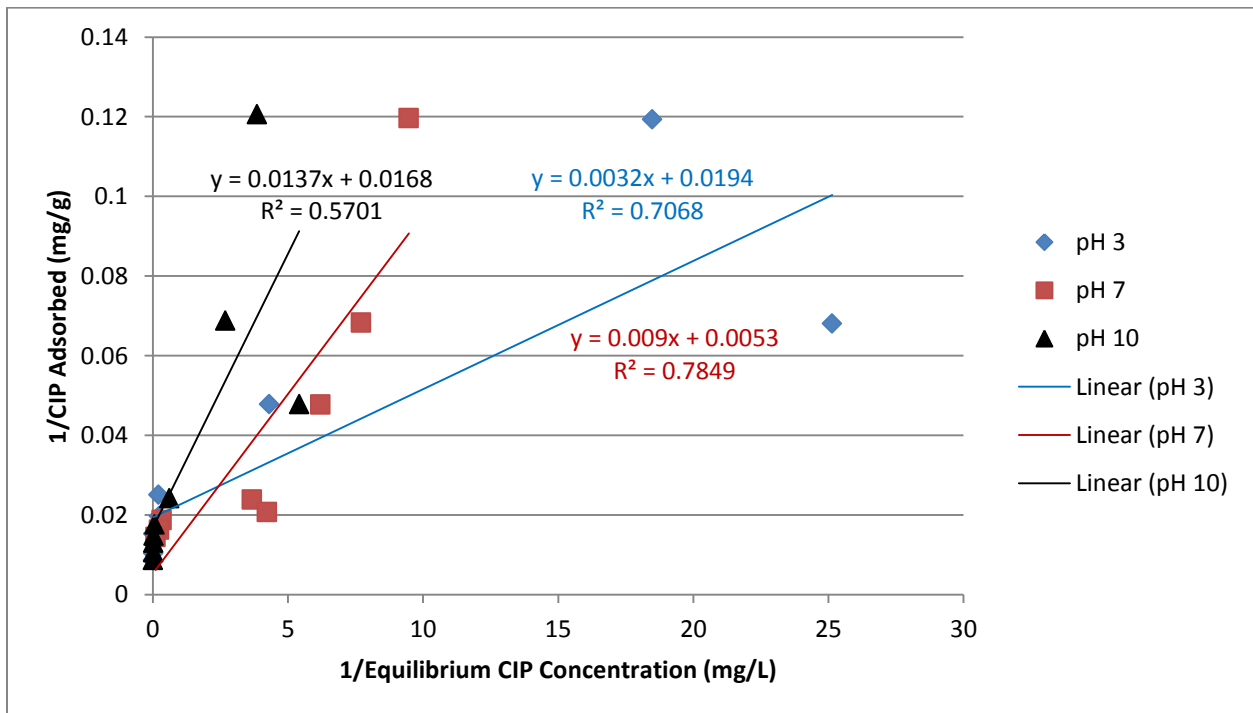


Figure 20: F600 Langmuir Isotherm

**F200**



**Figure 21: F200 Freundlich Isotherm**



**Figure 22: F200 Langmuir Isotherm**

# Adsorption Kinetics

## F600

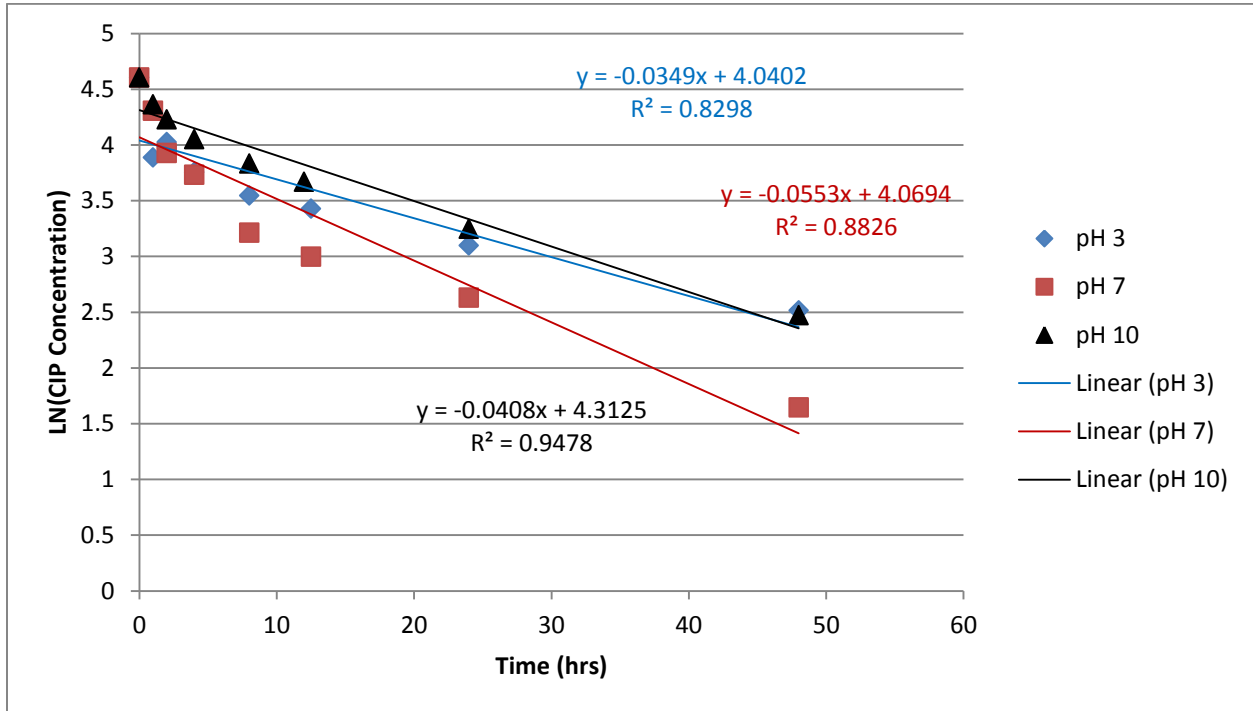


Figure 23: F600 1st Order Kinetics

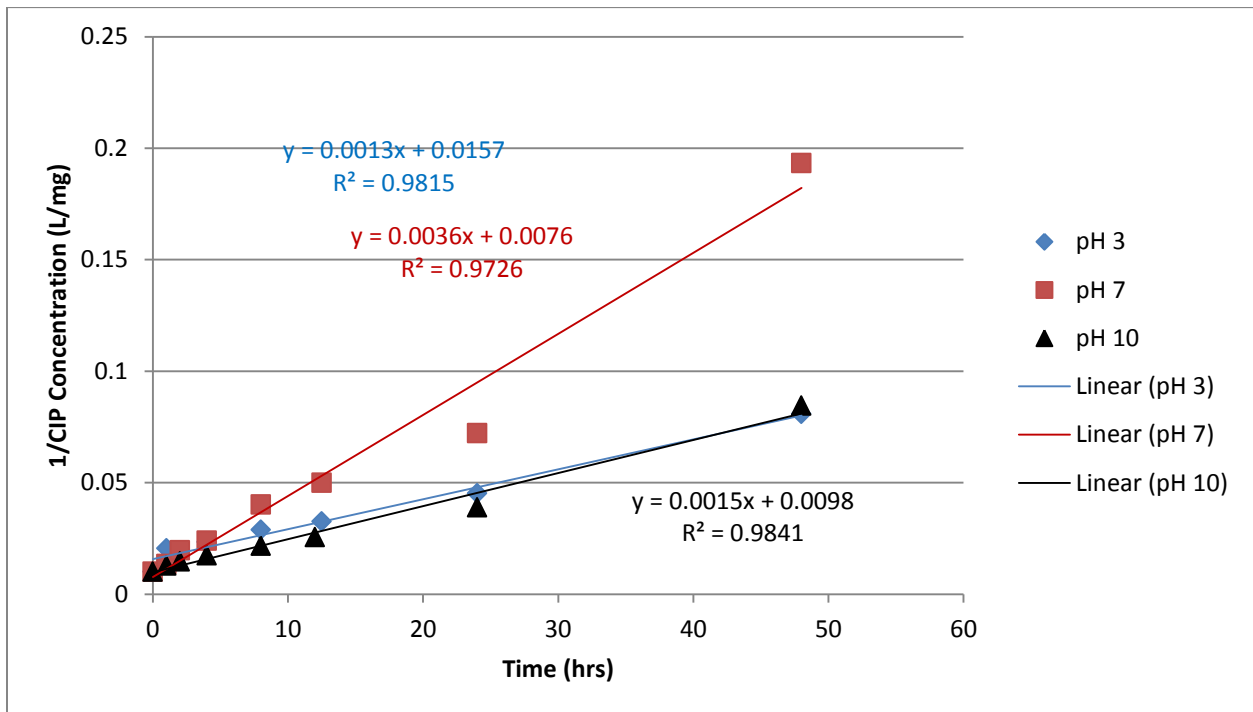


Figure 24: F600 2nd Order Kinetics

F200

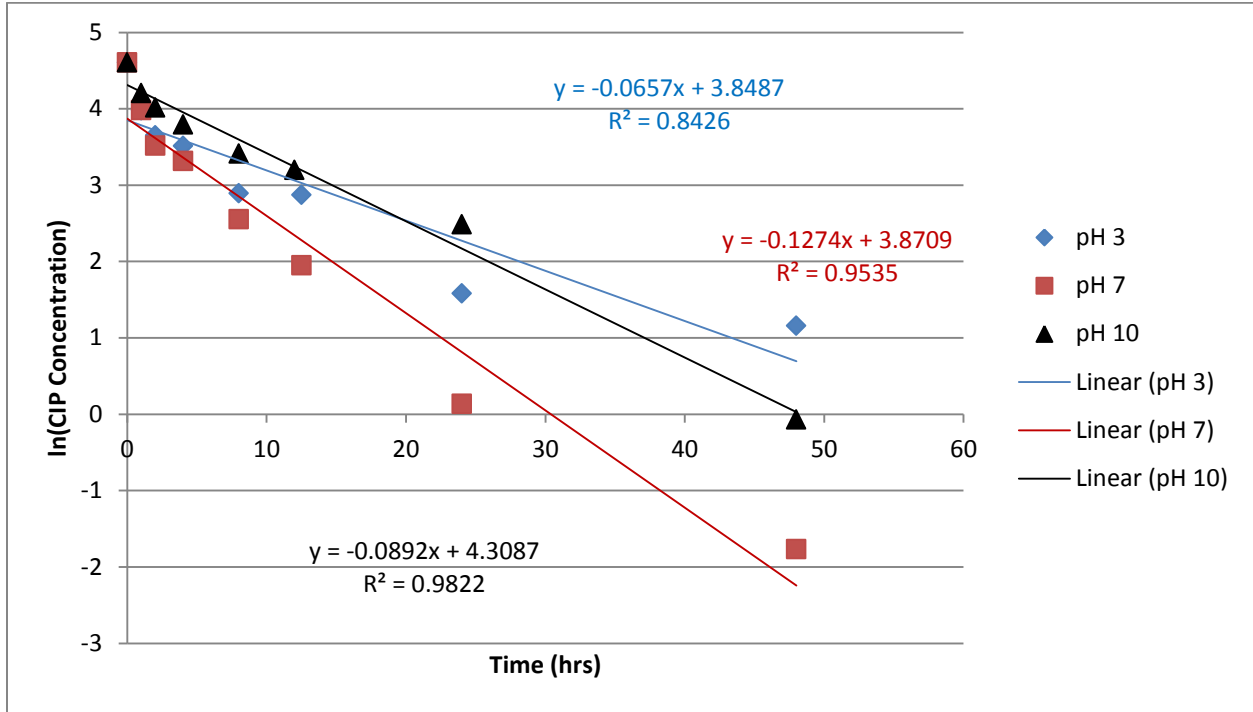


Figure 25: F200 1st Order Kinetics

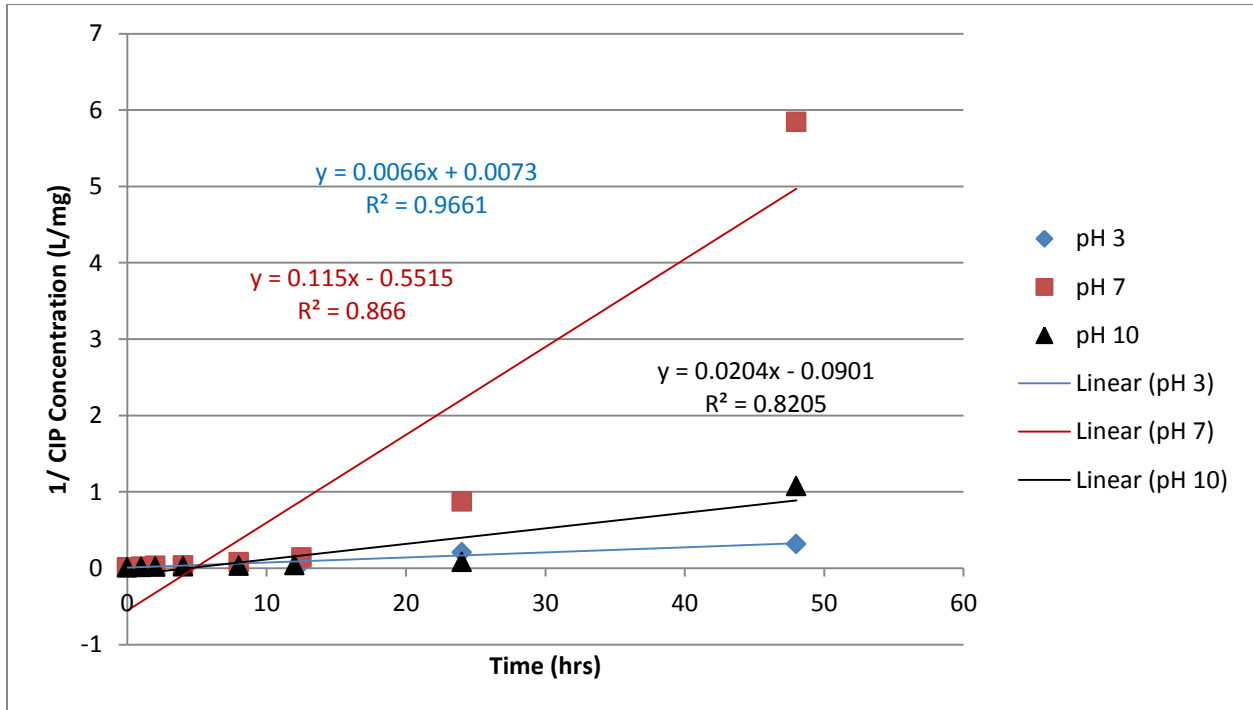



Figure 26: F200 2nd Order Kinetics

# Appendix D – GAC Data Sheets

## FILTRASORB® 200

### Granular Activated Carbon for Municipal Specifications



**Description**

FILTRASORB® 200 is a granular activated carbon developed by Calgon Carbon Corporation for the removal of taste and odor compounds, disinfection by-products, low level volatile organic compounds, and other targeted compounds from potable water. Although this product can be used for surface water applications with low level background total organic carbon, it was specifically developed for groundwater applications.

This activated carbon is manufactured from selected grades of bituminous coal to produce a durable granular product capable of withstanding the abrasion associated with repeated backwashing, air scouring, and hydraulic transport. Activation is carefully controlled to produce a product with a significant volume of high energy pores as measured by the trace capacity number, while still maintaining a high iodine number for effective adsorption of a broad range of high and low molecular weight organic contaminants. The higher density of this activated carbon results in a greater adsorptive capacity per filter volume as measured by the volume iodine number. The product is also designed to comply with all the applicable provisions of the AWWA Standard for Granular Activated Carbon, edition B604-05, the stringent extractable requirements of ANSI/NSF Standard 61, and the Food Chemicals Codex.

**Specifications**

| Specifications                         | Value          |
|--|----------------|
| Iodine Number.                         | 850 mg/g (min) |
| Moisture by weight                     | 2% (max)       |
| Effective size                         | 0.55 - 0.75 mm |
| Uniformity Coefficient                 | 1.9 (max)      |
| Abrasion No.                           | 75 (min)       |
| Trace Capacity Number                  | 11 mg/cc (min) |
| Screen Size by weight, US Sieve Series |                |
| On 12 mesh                             | 5% (max)       |
| Through 40 mesh                        | 4% (max)       |

**Features**

|  |  |
|--|--|
| Bituminous-based raw material                              | Provides higher hardness relative to other raw materials reducing the generation of fines and product losses during backwashing. |
| Coal is pulverized and reagglomerated with suitable binder |  |

**Benefits**

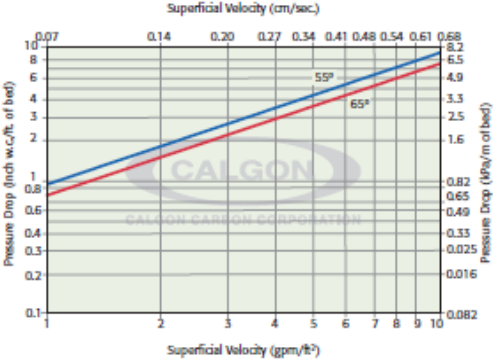
Pore structure provides a product with a significant volume of high energy pores as measured by the trace capacity number, while still maintaining a high iodine number.

Has a high density resulting in a greater adsorption capacity per filter volume, wets readily, and does not float, thus minimizing loss during backwash operations.

Creates optimal transport paths for faster adsorption.

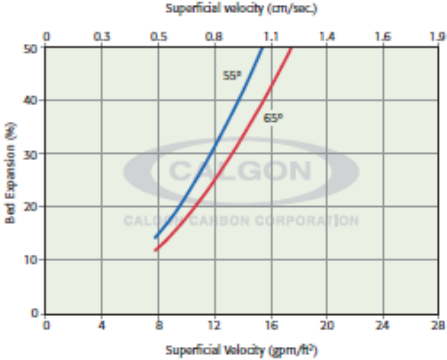
**Pressure Drop**

*Based on Backwashed and Segregated Bed*



**Backwash Bed Expansion**

*Based on Backwashed and Segregated Bed*



Making Water and Air Safer and Cleaner

Figure 27: F200 Data Sheet (Calgon Carbon Corporation, 2011)

63

# FILTRASORB® 600

## GAC for Trace Removal Applications



### Description

FILTRASORB® 600 is a high grade granular activated carbon manufactured by Calgon Carbon Corporation and optimized for superior performance in the removal of trace level organics from water. This carbon is manufactured from premium grades of bituminous coal to maximize the distribution of high energy adsorption pores in the carbon structure. The amount of high energy pores, as measured by the Trace Capacity Number, directly relates to the carbon's ability to adsorb organic contaminants at low concentrations.

As a high grade bituminous coal-based product, FILTRASORB® 600 possesses the durability required in many water treatment applications and is capable of withstanding the abrasion and dynamics associated with repeated reactivation, hydraulic transport, backwashing and mechanical handling. FILTRASORB® 600 is formulated to comply with all the applicable provisions of the AWWA Standard for Granular Activated Carbon, edition B604-05, the stringent extractable metals requirements of ANSI/NSF Standard 61, and the Food chemicals Codex.

### Specifications

| Specifications                         | Value          |
|--|----------------|
| Iodine Number                          | 850 mg/g (min) |
| Moisture by weight                     | 2% (max)       |
| Abrasion No.                           | 80 (min)       |
| Trace Capacity Number                  | 16 mg/cc (min) |
| Screen Size by weight, US Sieve Series |                |
| On 12 mesh                             | 5% (max)       |
| Through 40 mesh                        | 4% (max)       |

### Typical Property

| Typical Property | Value     |
|------------------|-----------|
| Apparent Density | 0.65 g/cc |
| Ash by weight    | 6%        |

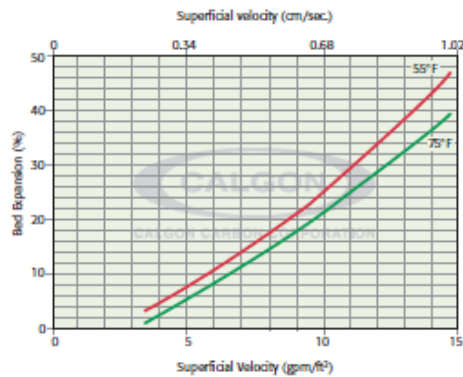
### Features

|  |   |
|--|---|
| Superior and consistent trace removal capacity               | Longer bed life between carbon exchanges.<br>Reduced down time.<br>Reduced operating costs.<br>Predictable system performance from one carbon bed to the next.<br>Reduces the likelihood of premature breakthrough. |
| Bituminous-based raw material                                | Rapid wetting, lack of floaters.  |
| High density   | Reduced losses during backwashing.<br>Generates the hardness and abrasion resistance required for thermal reactivation and minimizes generation of fines in operations requiring backwashing.                       |
| Coal is pulverized and reagglomerated with a suitable binder | Creates optimal transport paths for faster adsorption.  |

### Benefits

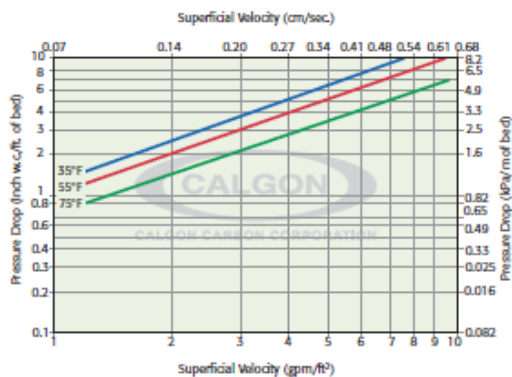
### Bed Expansion

Based on backwashed and segregated bed



### Pressure Drop

Based on backwashed and segregated bed



Making Water and Air Safer and Cleaner

Figure 28: F600 Data Sheet (Calgon Carbon Corporation, 2011)